

Climatological Study on Characteristics of Spring Dust Outbreaks
in East Asia and their Controlling Factors

東アジアにおける春季ダストの特徴とその要因に関する気候学的研究

WU, Jing

(武 靖)

A dissertation for the degree of Doctor of Environmental Studies

Department of Earth and Environmental Sciences,

Graduate School of Environmental Studies, Nagoya University

名古屋大学大学院環境学研究科地球環境科学専攻学位論文 博士（環境学）

2016

Abstract

Dust outbreaks occur frequently in arid and semi-arid regions of East Asia. The distribution and frequency of dust outbreaks experienced spatial and inter-annual variations. However, there are few reports on the recent changes of characteristics of dust emission in East Asia.

Dust emission, resulting from wind erosion in the source regions, is controlled by two major factors; erosivity (i.e., wind speed) and erodibility (i.e., land surface conditions). Erodiability is represented by an index of dust outbreak ratio, which was defined as the ratio of dust outbreak frequency and strong wind frequency. Erodiability factors include a number of land surface parameters that interact in complicated manners. Thus, to what extent each of the factors contributes to dust outbreaks, which varies regionally and seasonally, remains unclear. This study is aimed to understand the recent trend in spring dust emission, its erosivity and erodibility between 1999 and 2013 in East Asia.

Generally, dust outbreaks occurred more frequently in Mongolia than in northern China. The spatial distributions were investigated to understand changes in source regions for dust outbreaks. Between 2000 and 2003, the occurrence of dust outbreaks was more frequently in northern China than in Mongolia. Large positive anomalies of strong wind were distributed in northern China during this period, and large positive anomalies of dust outbreak ratio were also found for the period of 2000 to 2002. Since the year 2004, the occurrence of dust outbreaks in northern China revealed a decreasing trend except for the year 2006 when frequent strong wind occurred. During the study period, the distribution of frequent dust outbreaks in Mongolia was widespread to the east, along with a slight increasing trend in the strong wind. The steppe region appeared

to be a potential dust source region. The results suggest that the source region for Asian dust shifted from northern China to Mongolia.

To understand the change of source regions for Asian dust, the present study identified relative contributions of the erosivity and various erodibility parameters to inter-annual dust variations on a station basis during the period 1999-2013. A novel map of the controlling factor for dust emission in East Asian was presented in the present paper.

Erosivity (i.e., strong wind) controls the dust outbreaks in the Taklimakan Desert, west of the Hexi Corridor, and on the north side of the Altai Mountain. On the other hand, dust outbreaks are dependent on erodibility in steppe regions: lower precipitation or smaller vegetation of the previous summer was found to be related to dusty springs in the Mongolian steppe, whereas the smaller spring vegetation and less snow cover enhanced dust emission in the Inner Mongolian steppe. Anthropogenically restored vegetation in desertified areas was found to be likely to suppress dust emission in the Loess Plateau.

The effect of anthropogenic factors (e.g., grazing) on vegetation in Inner Mongolia is discussed. The current study suggests that the expansion of fenced grassland areas, and a plateauing of the amount of land being cultivated and the livestock population were related to the increase in the NDVI, especially from 2007 to 2013, which in turn was responsible for the recent decline in the frequency of dust outbreaks. Since climate change could be contributing to desertification, data of Abaga-qi, a county in Xilingol League of Inner Mongolia is further discussed. The results suggest that the summer vegetation in the typical steppe area was controlled by precipitation. However, the increasing trend in spring vegetation was greatly affected by

the protection of vegetation by the policy of dederring spring grazing in Inner Mongolia.

論文要旨

ダストストームは、東アジアの乾燥・半乾燥地域でしばしば発生する。発生源地域におけるダスト発生の分布と頻度は、時間的にも空間的にも変動する。その変動は、風下の日本や韓国の大気環境に大きな影響を与える。しかしながら、東アジアにおけるダスト発生の最近の傾向に関しては、ほとんど研究が行われていない。

本研究は、1999-2013年の東アジアの春季におけるダスト発生の傾向、および侵食能と受食能の空間分布を明らかにすることを目的とする。風食によって生じるダスト発生は、二つの要因、すなわち侵食能（風速）と受食能（地表面状態）に支配される。受食能は、複雑な地表面状態に依存する。本研究では、受食能を強風発生頻度に対するダスト発生頻度の比、すなわちダスト発生比で定義した。

まず、東アジアにおけるダスト発生の傾向を調べた。2000-2003年、ダスト発生は、モンゴルよりも中国北部で多かった。この期間、強風の大きな正偏差が中国北部に分布し、さらにダスト発生比の大きな正偏差も見られた。2004年以降、中国北部でのダスト発生は、減少傾向にある（2006年を除く）。一方、モンゴルにおけるダスト発生頻度の分布は、強風の増加傾向と共に、東側に向けて大きく広がった。草原地域は、ダスト発生源になる可能性を秘めている。これらの結果は、ダスト発生源の中心が中国北部からモンゴルに移動したことを示す。

以上の解析をふまえて、本研究では、東アジアにおけるダスト発生を支配するパラメーターに関する新しい地図を提案する。この地図は、1999-2013年の気象台データと衛星データをもとに、侵食能と受食能がダスト発生に寄与する相対的割合を求め、図化したものである。侵食能（強風）は、アルタイ山脈北部、タクラマカン砂漠北部、河西回廊西部において、主要な支配要因になっている。これらの地域は極度に乾燥した砂漠地域である。一方、草原地域では、ダスト発生は受食能（地表面状態）に依存している。

これらの地域では、前年夏季の少雨と貧弱な植生が草原における春季ダストの発生を強める。黄土高原では、砂漠化地域において人工的に回復された植生がダスト発生を抑制している。内モンゴルでは、フェンス付き草原面積、耕地面積、家畜頭数などの人為的要因が植生に影響を及ぼす。

本研究は、長期間の気象データと衛星データを用いて、東アジアにおける春季のダスト発生の特徴と支配パラメーターを気候学的に解明したものである。新しい成果として、ダスト発生を支配する侵食能と受食能の地図を提案した。

Contents

List of Figures

1. Introduction
2. Data and Methods
 - 2.1 Study region
 - 2.2 Surface meteorological data
 - 2.2.1 Present weather
 - 2.2.2 Strong wind
 - 2.2.3 Dust outbreak ratio
 - 2.2.4 Precipitation
 - 2.3 Land surface condition
 - 2.3.1 NDVI
 - 2.3.2 Snow Cover
3. Recent changes of dust occurrence, its erosivity and erodibility
 - 3.1 Dust outbreaks
 - 3.2 Erosivity and erodibility
 - 3.3 Erodibility factors
 - 3.3.1 Precipitation and vegetation cover
 - 3.3.2 Snow cover
4. Controlling factors of the recent dust occurrence in East Asia
 - 4.1 Data processing
 - 4.2 Controlling factors

4.2.1 Desert and desert-steppe region

4.2.2 Steppe region

4.2.3 Loess Plateau

5. Discussion

5.1 Dust source regions

5.2 Anthropogenic impacts in Inner Mongolia

6. Conclusion

Acknowledgements

References

List of Figures

Figure 1. Schematic diagram showing the relationship among the erosivity factor, erodibility factor, threshold wind (friction) speed, and wind erosion.

Figure 2. Land cover map of Dryland East Asia (DEA) in 2009, derived by the MODIS using the IGBP classification methods. DEA includes Mongolia (MG) and four provincial units (i.e., Inner Mongolia (IM), Xinjiang (XJ), Gansu (GX) and Ningxia (NX)) where grassland, desert, cropland and forests dominate the region (Qi et al., 2012).

Figure 3. Topography and distribution of SYNOP observation sites (dots and squares). Stations used in the present analysis are indicated by squares. An alphabet in a square indicates the region name; “A” (Altai Mountain), “N” (Northern Mongolia), “K” (Khangai Mountain), “C” (Central Mongolia), “E” (Eastern Mongolia), “G” (Gobi Desert), “T” (Taklimakan Desert), “S” (Tsaidam), “H” (Hexi Corridor), “L” (Loess Plateau), “I” (Inner Mongolia), and “P” (North Plain).

Figure 4. Spatial distributions of the mean DOFs in April for the period of (a) 1999-2013, and for (b) 1999, (c) 2000, (d) 2001, (e) 2002, (f) 2003, (g) 2004, and (h) 2005, respectively.

Figure 5. Spatial distributions of the mean DOFs for (a) 2006, (b) 2007, (c) 2008, (d) 2009, (e) 2010, (f) 2011, (g) 2012, and (h) 2013, respectively.

Figure 6. (a) Spatial distribution of the changing trend slope in the mean DOF in April from 1999 to 2103, and (b) inter-annual variations of the average DOF in April of the stations located in Mongolia, and China, respectively, during the period 1999-2013.

Figure 7. Spatial distributions of (a) the mean SWFs in April during the period 1999-2013, and spatial distributions of anomalies of the SWFs for (b) 1999, (c) 2000, (d) 2001, (e) 2002, (f) 2003, (g) 2004, and (h) 2005, respectively. The red and blue squares indicate positive and negative anomalies, respectively.

Figure 8. Spatial distributions of anomalies of the SWFs for (a) 2006, (b) 2007, (c) 2008, (d) 2009, (e) 2010, (f) 2011, (g) 2012, and (h) 2013, respectively. The red and blue squares indicate positive and negative anomalies, respectively.

Figure 9. Same as Fig. 7, but for the DOR

Figure 10. Same as Fig. 8, but for the DOR

Figure 11. Same as Fig. 7, but for the summer precipitation (June to August) during the period of 1998 to 2012.

Figure 12. Same as Fig. 8, but for the summer precipitation.

Figure 13. Same as Fig. 7, but for the annual maximum NDVI for the period of 1998 to 2012.

Figure 14. Same as Fig. 8, but for the annual maximum NDVI.

Figure 15. Same as Fig. 7, but for the NDVI in April for the period of 1999 to 2013.

Figure 16. Same as Fig. 8, but for the NDVI in April.

Figure 17. Same as Fig. 7, but for the snow fraction in March for the period of 2000 to 2012.

Figure 18. Same as Fig. 8, but for the snow fraction in March.

Figure 19. Same as Fig. 7, but for the snow fraction in April for the period of 2000 to 2012.

Figure 20. Same as Fig. 8, but for the snow fraction in April.

Figure 21. Inter-annual variations of (a) DOF, SWF, DOR in April, (b) NDVI in April

and snow coverage in March and April during the period 1999-2013 and (c) summer precipitation (June to August) and annual maximum NDVI during the period 1998-2012 at Hovd, Mongolia..

Figure 22. Plot of the DOF and (a) SWF, and (b) DOR in April 1999-2013 at Hovd.

Figure 23. Same as Fig. 15 except for the station Kashi, Xinjiang.

Figure 24. Same as Fig. 16 except for the station Kashi, Xinjiang.

Figure 25. Same as Fig. 15 except for the station Naran-bulag, Inner Mongolia.

Figure 26. Scatter diagrams for (a) DOF and SWF, (b) DOF and DOR in April 1999-2013; DOR and (c) NDVI in April, (d) annual maximum NDVI and (e) summer precipitation (June to August) in the previous year, and (f) snow cover in March at Naran-bulag, Inner Mongolia.

Figure 27. Same as Fig. 19 except for the station Choir, Mongolia.

Figure 28. Same as Fig. 20 except for the station for the station Choir, Mongolia.

Figure 29. Map of the controlling factors for dust emission in East Asia. The stations, where erosivity shows statistically significant correlation with the DOF at 5% confidence level are shown in red squares. The stations, where erodibility shows a stronger correlation with the DOF are shown in blue triangles. The stations, where spring snow cover, spring NDVI, annual maximum NDVI and precipitation in the previous summer controls DOR, are shown by “S” , “A” , “M” , or “P” , respectively at 5% (red) and 10% (black) confidence level. Background color illustrates altitude

Figure 30. Spatial distributions of aeolian desertified land in Northern China in 1950s, 1987, and 2000. Due to restoration policy, the desertification was reversed in some areas in the Northern China by the end of 1990s. Human activities have also pushed the agro-pastoral boundary northwards by approximately 200 km from 1950s to 2000

(Wang et al., 2008a).

Figure 31. Spatial distributions of the changing trend slope in summer NDVI from 1998-2012. An increasing (decreasing) trend is presented by red (blue) color in background.

Figure 32. Inter-annual variations of (a) DOF, SWF, DOR in April, (b) NDVI in April and snow coverage in March during the period 1999-2013 and (c) summer precipitation (June to August) and annual maximum NDVI during the period 1998-2012 for the 19 stations in Inner Mongolia.

Figure 33. Same as Fig. 20 except for the station for the mean values of the 19 stations in Inner Mongolia.

Figure 34. Inter-annual variations of (a) fenced grassland areas, (c) total cultivated land area and (d) the total number of sheep and goats at the end of the year, 1998-2012 in Inner Mongolian, and (b) plot of the April NDVI and the total area of fenced grassland in Inner Mongolia. Arrows in (c) and (d) indicate a plateauing of the variables. (Data source: Inner Mongolian Statistical Yearbook, 1999-2013).

Figure 35. Administrative map of Xilingol League

Figure 36. Vegetation map of the Xilingol grassland region, Inner Mongolia, China, showing the spatial pattern of major ecosystem types present in the 1960s–1970s (redrawn from Hou 2001)

Figure 37. Distributions of the ratio of fenced grassland in Xilingol League in 2005 (a), and 2012 (b), respectively; and sheep unit in 2005 (c), and (d), respectively.

Figure 38. Inter-annual variations of (a) NDVI and precipitation in summer between 1998 and 2012, (b) NDVI and temperature in April between 1999 and 2013, and (c) the ratio of fenced grassland to the total grassland and the number of sheep unit at year end

during the period 1998-2012 at Abaga Qi.

Figure 39. Scatter diagrams for (a) annual maximum NDVI and summer precipitation, NDVI in April and (b1) temperature in April, (b2) an annual maximum NDVI at Abaga Qi.

Figure 40. Scatter diagrams for the NDVI in April and (a) the ratio of fenced grassland to the total grassland, and (b) sheep unit at Abaga Qi.

1. Introduction

Aeolian dust has a number of environmental effects, for example, on air pollution, on the health of humans and livestock, and on the climate (Miller and Tegen, 1998; Wang et al., 2005). Arid and semi-arid regions in East Asia are the main dust sources for Asian dust. The emitted dust particles are entrained into the atmosphere and transported to downwind regions such as Japan, Korea and even as far as the northwestern Pacific (e.g., Iwasaka et al., 1983; Hara et al. 2006). Such research suggested that Asian dust is not only a local but also a global environmental issue.

Many global models have been developed to simulate a series of processes; dust emission, transport and deposition (e.g., Ginoux et al., 2001; Woodage et al., 2010). Due to a lack of observational evidence of land surface characteristics and understandings of how the characteristics impact dust emission, there still exist uncertainties in simulating dust emission processes (e.g., Uno et al., 2006; Todd et al., 2008).

Previous studies have classified five regions as main dust sources: the Taklimakan Desert (Tarim Basin) in the western China, the Gobi Desert in the southern Mongolia and the northwest of Inner Mongolia, the Hexi Corridor, the Loess Plateau, and the east of Inner Mongolia by analyzing synoptic reports (e.g., Sun et al., 2001), remote sensing images (e.g., Prospero et al., 2002), model simulations (e.g., Zhang et al., 2003).

Wang et al. (2008b) analyzed the meteorological data of dust events in China for the period 1960-2004 and suggested that Taklimakan Desert was one of the major sources for dust storms. Located in the south edge of the Taklimakan Desert, the Hetian station had the highest frequency of dust storms (47%) between 1998 and 2003. Goudie and Middleton (1992) also reported a high frequency of 32.9 dust storm days per year at Hetian during the period 1954-1980. The long-term trends in dust storms have been

studied by Zhu et al. (2008). They pointed out that the most frequent dusty years in the Taklimakan Desert appeared in the 1950s, and then it showed a decreasing trend from the 1980s.

Dust storms in Mongolia were most frequently observed in the southern Gobi Desert as reported by Natsagdorj et al. (2003). The Gobi Desert in southern Mongolia and northern Inner Mongolia has been suggested as one of the dominant dust sources based on synoptic analyses of dust storm reports over the period 1960-1999 by Sun et al. (2001). They also suggested that the most frequent dust storms occurred in the 1970s. Similar with the trend in the Taklimakan Desert, dust storm in the Gobi Desert showed a decrease since the 1980s (Wang et al., 2008b). An increase in the occurrence of dust events in Mongolia and parts of northern Inner Mongolia was found during the period 1998-2007 in Lee and Sohn (2011); whereas, a decrease in 2003-2004 was also found by Lee and Kim (2012). However, a peak in the frequency of dust events in 2000-2002 has been reported in a number of previous studies (e.g., Kurosaki and Mikami 2003). Shao and Wang (2003) demonstrated that dust events frequently occurred in the Gobi Desert were severe and widespread. Japan and Korea also experienced an increase in the occurrence of dust events between 2000 and 2002, suggesting that dust emission in the Gobi Desert has a widespread impact on dust events in eastward downwind regions (e.g., Kimura 2012b; Kim 2008). Zhang et al. (2008) suggested that dust from this region may be also transported southeastward, such as to the Loess Plateau.

By analyzing surface observations of dust storm in China, Wang et al. (2004) reported two dust source regions: one is the Taklimakan Desert, and the other is the west Inner Mongolian Plateau, including the Hexi Corridor and northwest of the Loess Plateau. This region has been identified part of the target source region for the dust

events over Japan (Kimura 2012a). The highest frequency of dust storm in China during the period 1960-1999 was the Hexi Corridor (Sun et al., 2001). The Minqin station located in the Loess Plateau had frequent dust observations since the 1950s. The mean frequency of dust storm at Minqin was 37.3 days per year for the period 1954-1980 (Goudie and Middleton, 1992), and was 28.1 days per year for the period 1954-2000 (Wang et al., 2005). A dusty belt has been revealed in the Hexi Corridor between 1998 and 2003 by Shao and Dong (2006). They suggested that a second dusty belt existed in parallel with the Hexi Corridor. The Loess Plateau was located in this belt.

Qian et al. (2004) indicated the eastern Inner Mongolia was a major dust source for dust storms in China between 1954 and 1998. The annual variation showed a high dust frequency in the mid-1960s and decreased afterward. However, Dust emissions in part of this region have been increasing between 1960 and 1999 (Zhang et al., 2003). Extending the study period to 2007, Zhu et al. (2008) suggested that there was no decreasing trend in the eastern Inner Mongolia, and dust storms originating from this region may have impact on the dust events in downwind regions. Combining part of the neighboring area in Mongolia, this region was the biggest contributor (42%) to long-range dust transport during 2000-2006 by analysis of the MODIS monitoring data (Zhang et al., 2008).

Inter-annual variation can be seen in the frequency of Asian dust originating in those dust source regions and shows various characteristics from region to region. However, there was little report on the spatial and temporal variation in dust event frequency in recent years, especially after 2007. There also exists a debate on which factor is primarily responsible for the distributions of dust sources; climate change or human activities

Dust emission, resulting from wind erosion, is dependent on aeolian erosivity (hereinafter, erosivity) and aeolian erodibility (hereinafter, erodibility) (UNEP, 1997) (Fig. 1). Erosivity is the ability of wind forces to erode existing soil, and is controlled primarily by wind strength. The erosivity factor is simply expressed by wind speed, and its relation to dust emission has been widely studied (e.g., Kurosaki and Mikami, 2003). A significant decline from the 1950s to the early 1990s, especially from the mid-1980s, in the Gobi Desert and northern China was found to be closely related to the reduction in cyclone activity, which caused a decrease in the frequency of strong wind (e.g., Qian et al. 2002; Wang et al. 2008b). The significant effect of strong wind on dust outbreaks has been found in the Taklimakan Desert (Kim and Kai, 2007). Strong wind, which is the driving force to cause dust storms, is majorly formed by synoptic scale cyclones around the Gobi Desert (e.g., Takemi and Seino, 2005), and is majorly formed by gravity current associated with mesoscale cold front in the Taklimakan Desert (e.g., Aoki et al., 2005). The special geography in Hexi Corridor provides a favourable condition to accelerate wind speed (Ci and Yang, 2010), thus forming the preferential route of dust transportation (Shao and Dong, 2006).

Erodibility is the susceptibility of soil and land surface to wind erosion, which, with some exceptions, has not been well measured or quantified over a broad area (Kurosaki and Mikami, 2007; Kurosaki et al., 2011b). Erodibility is influenced by various factors, such as vegetation coverage, snow cover, and soil moisture. These factors are characterized by substantial seasonal, inter-annual and spatial variations. In general, spring is the dust season in East Asia, while its seasonal changes are strongly controlled by drastic changes in land surface conditions. For example, in spring, frozen ground increased the threshold wind speed for dust emission in the East Mongolian

Plateau (Han et al., 2011). Abulaiti et al. (2014) pointed out that the freeze–thaw cycle during spring resulted in a lower threshold wind speed for dust emission on the desert steppe of Mongolia, whereas Ishizuka et al. (2012) suggested that the destruction of the crust on the surface in the spring reduced the threshold wind speed in the same site.

As for the inter-annual variations of dust, Zou and Zhai (2004) and Liu et al. (2004) demonstrated that the abundant spring vegetation resulted in a decline in dust frequency in Inner Mongolia during the period of 1982 to 2001. Lee and Kim (2012) revealed that the occurrence of dust outbreaks was reduced by spring snow coverage in Inner Mongolia and Gobi desert, and by spring vegetation in the Loess Plateau during the period of 1996 to 2007. The deterioration of surface vegetation and a reduction in snow cover has resulted in an increase in the frequency of dust events in 2000-2002 in northern China (Xu et al. 2006; Kurosaki and Mikami 2005).

The land surface memory in Mongolian grasslands was investigated by Shinoda and Nandiatsetseg (2011). They showed that soil moisture and vegetation anomalies determined by summer precipitation were maintained during the winter, affecting dust occurrence in the following spring. Nandiatsetseg and Shinoda (2015) also pointed out that the standing dead grasses had the most significant impact on spring dust emission. Kurosaki and Mikami (2005) reported the spatial distributions of threshold wind speed, which can be used as an index of erodibility. The threshold wind speed was the lowest in the Taklimakan Desert, and the highest in northern Mongolia.

Some researchers believe that desertification resulted in formation of the newly source regions for dust emission (e.g., Ji and Zhao, 2001; Wang et al., 2004). Desertification is defined as “land degradation in arid, semi-arid and dry sub-humid areas resulting from various factors, including climatic variations and human activities”

(Assembly 1994). Aeolian desertification is one type of desertification, and is characterized by wind erosion, which is related to the occurrence of dust events. The vast man-made forests may have impact on a decrease of dust storms in northern China (Parungo et al., 1994). Tan and Li (2015) have suggested that the “Green Great Wall” program increased vegetation coverage and reduced the dust event frequency in northern China from the 1970s to 1990s. Wang et al. (2008a) have suggested that there has been a continuous reduction in aeolian desertification in arid and semi-arid China from the 1990s to 2004. However, a renewed increase in the rate of aeolian desertification has been identified as a possible cause of the increase in dust events in the 2000s (e.g., Chen and Tang 2005). Other researchers argued that modern desertification mainly caused by human activities had little effect on dust emission. For instance, the contribution of anthropogenic desertification in China to Asia dust emission was only about 6% for the period 1960-2002 as reported by Zhang and Gong (2005). The insignificant effect of desertification on dust emission was also suggested by using model simulation (Zhang et al., 2003). Therefore, further work is needed on the relation between desertification and dust emission, as well as possible mitigation strategies.

Given the above-mentioned background, substantial temporal and spatial variations in erosivity and erodibility manifested in East Asia should be related to those of dust emission by a systematic analysis with a full coverage of the area. Kurosaki et al. (2011a) suggested that changes in erodibility parameters of precipitation, soil moisture, and above-ground biomass significantly influenced dust outbreaks in April by using data at only one station for Mandalgobi, Mongolia. However, wider identification of the controlling factors for dust outbreaks has not been conducted over the entire arid and

semi-arid region in East Asia. In the present study, the author investigates inter-annual variations (1999-2013) of spring dust outbreaks as well as erosivity and erodibility over arid and semi-arid regions in East Asia. A novel map of the controlling factors for dust outbreaks is presented by identifying the relative contributions of erosivity and erodibility factors to recent inter-annual variations in dust occurrence on a station basis. This paper is organized as follows. Chapter 2 describes the meteorological and remote sensing data and the index of erodibility used in this study. In Chapter 3, the author investigated the recent trend in distribution and frequency of dust emission, its erosivity and erodibility, and erodibility parameters of vegetation cover, snow cover and precipitation over the arid and semi-arid regions in East Asia. In Chapter 4, the author examined relative contributions of erosivity and various erodibility factors to dust occurrence on a station basis. A map of the controlling factor for dust emission in East Asia was presented. Chapter 5 discusses the recent changes of source regions for Asian dust emission, and also discusses the influence of anthropogenic factors (e.g., grazing) on dust outbreaks in Inner Mongolia. Finally, Chapter 6 presents conclusions.

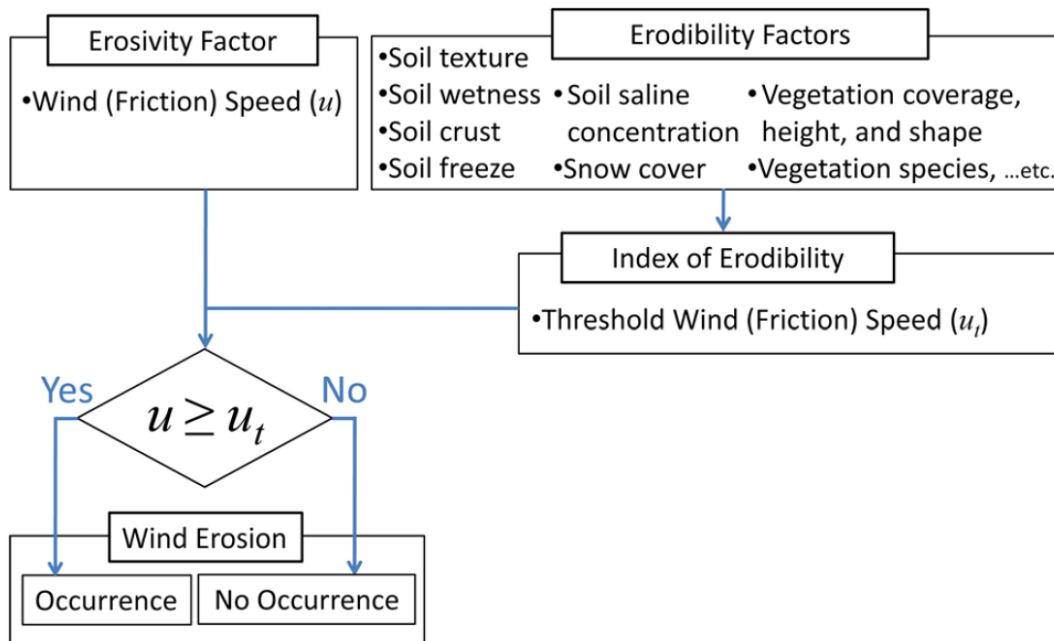


Figure 1. Schematic diagram showing the relationship among the erosivity factor, erodibility factor, threshold wind (friction) speed, and wind erosion.

2. Data and Methods

2.1 Study region

There are 40 SYNOP stations located in Mongolia and 162 SYNOP stations located in China over the arid and semi-arid regions in East Asia. The region includes Mongolia, part of Inner Mongolia Autonomous Region, Gansu Province, Shanxi and Qinghai Province, and also Ningxia Hui Autonomous Region. The land cover type of the study region is generally divided to desert, desert steppe, and steppe referring to the map as shown in Fig. 2 given by Qi et al. (2012). Referring to topography and the land cover classification, those stations are located in 11 regions as indicated by an alphabetic letter in the squares; “A” (Altai Mountain), “N” (Northern Mongolia), “K” (Khangai Mountain), “C” (Central Mongolia), “E” (Eastern Mongolia), “G” (Gobi Desert), “T” (Taklimakan Desert), “S” (Tsaidam), “H” (Hexi Corridor), “L” (Loess Plateau) and “I” (Inner Mongolia), as illustrated in Fig. 3.

2.2 Surface meteorological data

Data for dust occurrence and meteorological factors were extracted from 6-hourly World SYNOP reports, containing present weather codes, and information on wind speed and precipitation over the period 1999-2013. These variables are recorded four times a day (00, 06, 12, 18 UTC).

2.2.1 Present Weather

The World Meteorological Organization (WMO) classified present weather into 100 kinds (ww=00-99). All dust-related phenomena are called dust event, which are ww = 06, 07, 08, 09, 30, ... , 35 and 98. This study focuses on dust events originating in the study region, and does not consider floating dust (ww = 06), which is defined as

widespread dust in suspension in the air and may have migrated from outside the study region. This study investigated dust outbreaks, which are defined as dust in the production phase. Dust outbreaks are divided into (4) “blowing dust” (i.e., moderate dust outbreak), which are $ww= 07$ and 08 , and (5) “dust storm” (i.e., severe dust outbreak), which are $ww= 09, 30, \dots, 35$ and 98 . The frequency of dust outbreak (DOF) was defined as the percentage of days experiencing dust outbreaks during the observation period.

Lee and Kim (2012) and Kurosaki and Mikami (2005) have demonstrated that April has the peak DOF during the whole year. To focus on the most frequent dust occurrence, the author compiled the average DOF in April at each station, and excluded SYNOP stations for which the average number of dust outbreaks was less than one day per year. Analysis was conducted at the remained 66 SYNOP stations (squares in Fig. 3).

2.2.2 Strong Wind

SYNOP surface wind speed is observed at a height of 10 meters. Strong wind is defined as the wind speed exceeding a constant threshold wind speed. As commonly used for arid and semi-arid regions (e.g., Tegen and Fung, 1994), a value of 6.5 m/s is defined as the threshold wind speed in this study. The frequency strong wind (SWF) was defined in the same criteria with DOF.

2.2.3 Dust outbreak ratio

In this study, erodibility was described by an index - dust outbreak ratio (DOR), which was defined as the ratio of DOF to SWF. Normalized by strong wind, the index

indicates the possibility of dust occurrence at a given condition of wind. The DOR expresses the vulnerability of land surface condition to wind erosion. A high value of DOR indicates a vulnerable land surface, for which dust outbreaks tend to occur. Kimura and Shinoda (2010) used the same definition of dust outbreak ratio, but they used different definition of the SWF.

2.2.4 Precipitation

In arid and semi-arid regions, the seasonal variation of rainfall is quite unbalance. Summer is the season having more than half of the annual accumulated amount of rainfall during the whole year. Therefore, the total amount of summer precipitation from June to August was calculated and its persistent impact on spring dust outbreaks that occur in the following year was analyzed.

2.3 Land Surface Condition

2.3.1 NDVI

The normalized difference vegetation index (NDVI) is defined as:

$$\text{NDVI} = (\text{NIR} - \text{RED}) / (\text{NIR} + \text{RED}),$$

where NIR and RED are the reflectance measured in the near-infrared channel (0.78-0.89 μm) and the red channel (0.61-0.68 μm), respectively. The NDVI data used in this study were derived from SPOT VEGETATION images with 1km spatial resolution (<http://free.vgt.vito.be>). The NDVI data is computed from 10-day composites, and calculated using the maximal NDVI method to eliminate the effects of cloud cover and snow/ice (Veroustraete et al., 2005). To corresponding SYNOP meteorological data, the author made a spatial average on a station basis. The mean NDVI for the 50 \times 50

pixels surrounding the observation site was used.

2.3.2 Snow Coverage

Snow cover data were obtained from MODIS/Terra Snow Cover Daily L3 Global 0.05°CMG (MOD10C1) version 5 (Hall and Salomonson 2006). The dataset provides fractional snow cover in pixel based on the normalized difference snow index (NDSI) (Hall et al. 2002). The dataset was released in February 2000, so this study investigated monthly mean snow cover in March and April, 2000-2013, respectively. For measuring snow cover, the same region was calculated as used for the NDVI data, but with a lower resolution (10×10 pixels).

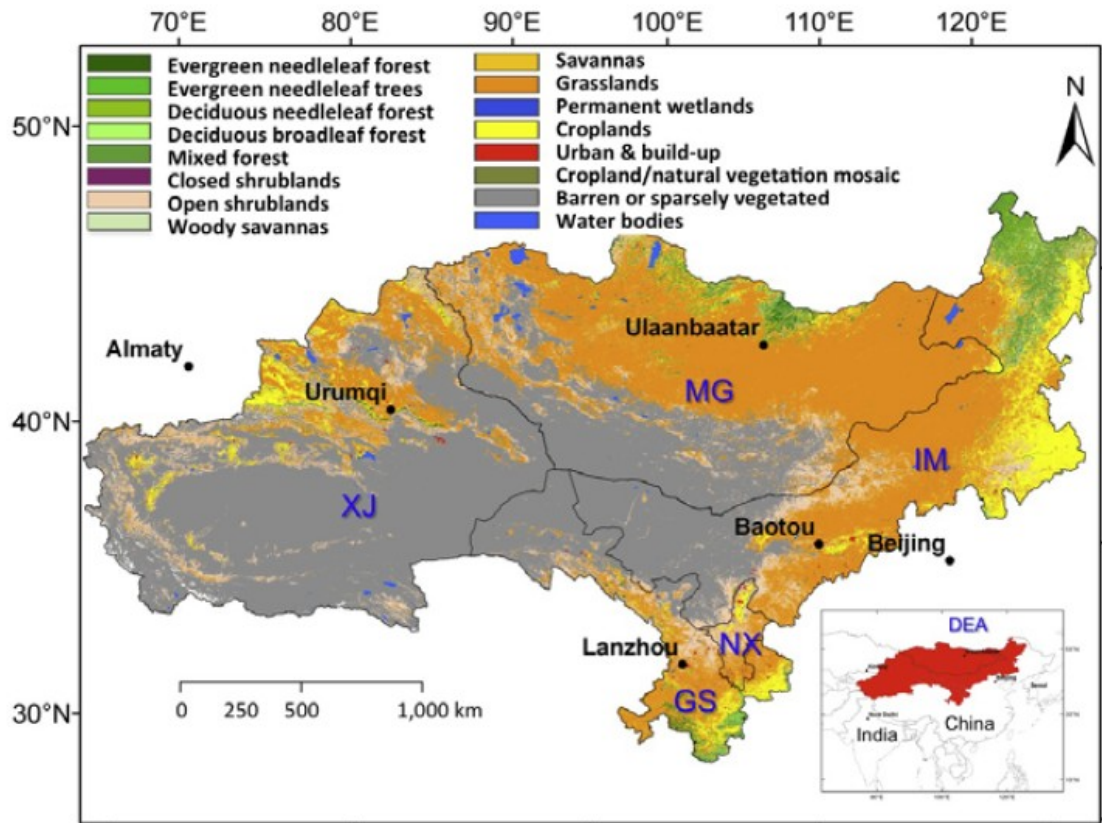


Figure 2. Land cover map of Dryland East Asia (DEA) in 2009, derived by the MODIS using the IGBP classification methods. DEA includes Mongolia (MG) and four provincial units (i.e., Inner Mongolia (IM), Xinjiang (XJ), Gansu (GX) and Ningxia NX) where grassland, desert, cropland and forests dominate the region (Qi et al., 2012).

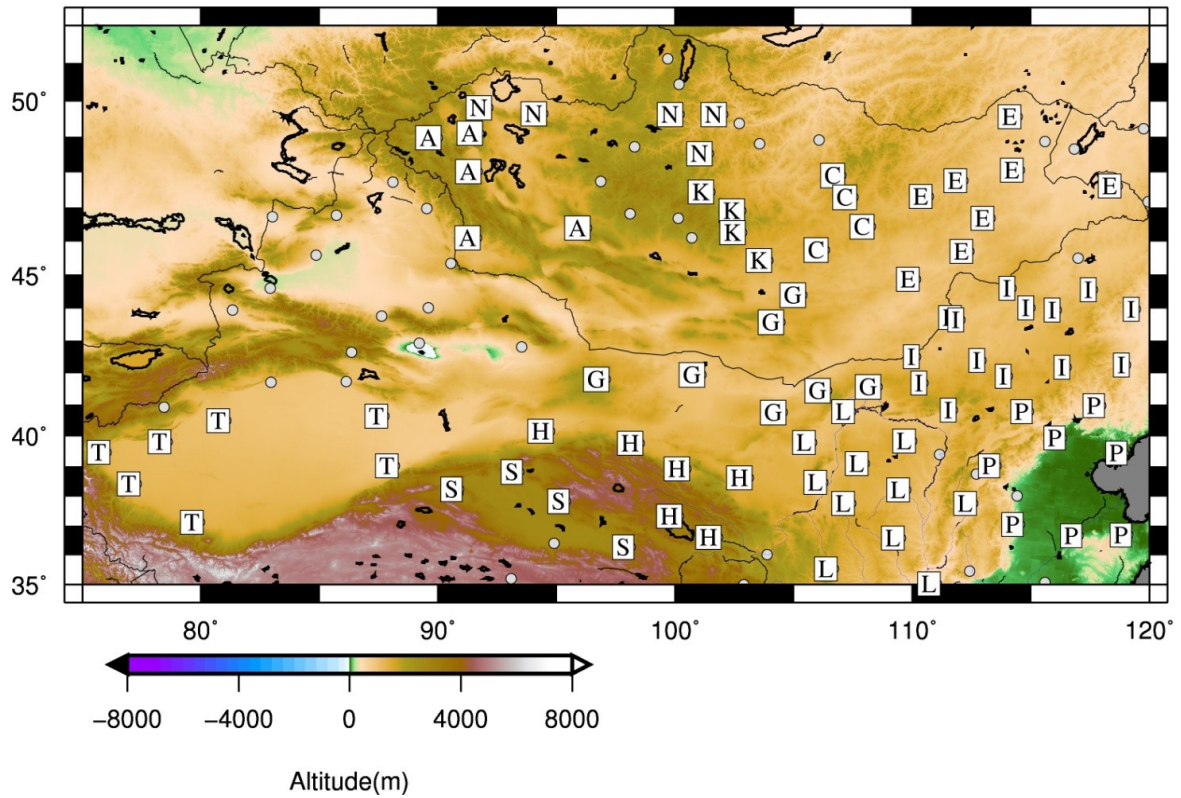


Figure 3. Topography and distribution of SYNOP observation sites (dots and squares). Stations used in the present analysis are indicated by squares. An alphabet in a square indicates the region name; “A” (Altai Mountain), “N” (Northern Mongolia), “K” (Khangai Mountain), “C” (Central Mongolia), “E” (Eastern Mongolia), “G” (Gobi Desert), “T” (Taklimakan Desert), “S” (Tsaidam), “H” (Hexi Corridor), “L” (Loess Plateau), “I” (Inner Mongolia), and “P” (North Plain).

3. Recent changes of dust occurrence, its erosivity and erodibility

3.1 Dust outbreaks

Figure 4a shows the average DOFs in April during the period from 1999 to 2013. The DOF occurred more frequently in Mongolia than in northern China. In Mongolia, stations located in the Gobi desert and in the eastern steppe have a relatively high value of the DOF. Figure 4b-h and Fig. 5a-h show the spatial distribution of the DOF. Between 2000 and 2003, the DOFs in northern China were higher than in Mongolia. In 2000, frequent dust outbreaks were observed in the Loess Plateau. The widest distribution of high values of the DOF was found in 2001, in the Gobi Desert located in the southern Mongolia and the northwest of Inner Mongolia the Loess Plateau, and the Hexi Corridor. The DOF in the Taklimakan Desert was not as high as that in the above mentioned regions, but reached to the peak value compared with that in the other years. For the period of 2001 to 2003, the DOF was high in the southern Gobi Desert in Mongolia. Since then, the DOF showed an increasing trend at most stations in Mongolia, and the DOF over the whole Mongolia region were higher than that in northern China. In the year 2004, high values of the DOF were also found in the northern side of the Khangai Mountain and in the east. Since the year 2005, frequent dust outbreaks were likely to have a wide distribution to the eastward (the steppe region). In northern China, the DOF was relatively high in Inner Mongolian and the Loess Plateau in 2006. After that, an obvious declining trend was seen at most stations in northern China, especially in the steppe region of the northeast Inner Mongolia.

Figure 6a shows the spatial distribution of the slope of trend in the mean DOF from 1999 to 2013. An increasing trend was found at most stations in the Mongolian steppe region, and in the west of the Altai Mountain region. However, in northern China,

the changes in the DOF at most stations show a decreasing trend. Figure 6b shows the time series of the average DOF of stations which are located in Mongolia and northern China, respectively. Between 1999 and 2003, the DOFs in Mongolia and northern China show similar variations, and the DOFs in northern China were higher. Since then, the DOFs in northern China show a general decreasing trend. However, the DOFs in Mongolia increased and show higher values than those in northern China.

3.2 Erosivity and erodibility

The SWF in April is averaged for the period 1999-2013 (Fig. 7a); and the spatial distributions for each year are shown in Fig. 7b-h and Fig. 8a-h. As shown in Fig. 7a, the mean spatial pattern indicates that strong winds were frequently observed in the Mongolian Plateau; including of the southeast of Mongolia and the north of Inner Mongolia. Low values of the SWF were distributed in the Altai Mountain, the Taklimakan Desert, the Hexi Corridor and the Loess Plateau. During the study period, large positive anomalies of the SWF over the study region were found in the years of 2001, 2002, and 2006. In 2003 and 2005, the SWF was high in northern China and in Mongolia, respectively. During the period of 2007 to 2011, there was a decreasing trend in the SWF at most stations over the study region. In the period 2012-2013, a slight increasing trend in the SWF was found in Inner Mongolia.

The erodibility index-DOR is averaged over the whole study period 1999-2013 (Fig. 9a), and the spatial distributions of anomalies are shown in Fig. 9b-h and Fig. 10a-h. Without information on wind speed or occurrence of strong wind at some stations, there were no data for the DOR. The highest mean DOR was observed in the Taklimakan Desert. The mean values of the DOR were also high in the Altai Mountain,

the Hexi Corridor and the Loess Plateau. Large positive anomalies of the DOR were found in the Hexi Corridor, the Loess Plateau, and Inner Mongolia during the period of 1999 to 2002. The positive anomalies of the DOR show a wide distribution in northern China in 2006 as shown in Fig. 12a. Since then, anomalies of the DOR in the northeast Inner Mongolia were tend to be steady with negative values. It indicates that the land surface condition has been improved to resist the wind erosion.

3.3 Erodibility factors

3.3.1 Precipitation and vegetation cover

As shown in Fig. 11a, the mean value of accumulated amount of summer precipitation (June-August) was from low to high, from the west to east. The precipitation amount was the lowest (< 70 mm) in the Taklimakan Desert, and was also low with the value of < 100 mm in the Gobi Desert and the Hexi Corridor. In those regions, the NDVI in summer was lower than 0.2 (Fig. 13a), indicating a bare land surface with less vegetation, especially in the Taklimakan Desert. The values of NDVI were much lower in the following spring (Fig. 15a).

Spatial distributions of the anomalies of the summer precipitation are shown in Figs. 11b-h and Fig. 12a-h. The values of anomalies at stations in Taklimian Desert and the Hexi Corridor, were relatively lower than in the other regions. Large positive anomalies in Taklimakan Desert were found in 2000, 2002, 2005, 2010, and 2012. In northern China, dry periods, with negative anomalies of the precipitation, were found to be in the years of 2000-2001, 2005, 2009-2011, while the wet years were 2002-2004, 2010, and 2012. The variations in values of anomalies in Mongolia were greater those in northern China. Large positive anomalies were found in the west side of Mongolia in

the years of 2001-2003; at some stations in the central steppe region in the years of 2001, 2003, 2006-2008, and 2011-2012; in the eastern steppe region in 2012.

Figure 13b-h, Fig. 14a-h, and Fig. 15b-h, Fig. 16a-h show that the variations in the annual maximum NDVI, and in the NDVI of the following spring generally have similar characteristics. Negative anomalies of the NDVI were widely distributed over the study region in summer between 1998 and 2002, and in spring between 1999 and 2003. Vegetation in the west of Mongolia and in the south side of the Inner Mongolian steppe region show an increasing trend for the period of 2003 to 2006 in summer. An increase in the summer NDVI was also found in the central steppe region of Mongolia for the period of 2006 to 2009. A wide distribution of large positive anomalies in the summer NDVI was found in the period of 2010 and 2012. In spring, positive anomalies of the NDVI in Mongolia were found in 2004, 2009, and 2012-2013. An increasing trend in the spring vegetation in northern China was found in the period of 2008 to 2009, and the period of 2011 to 2013.

3.3.2 Snow cover

The mean snow cover in March between 2000 and 2013 and the spatial distributions of anomalies for each year were shown in Fig. 17a-h and Fig. 18a-h. As shown in Fig. 17a, there was almost no snow cover in the Taklimakan Desert and the Loess Plateau. Snow cover was low, with less than 30% coverage, in the Gobi Desert. Large positive anomalies of snow cover in March in the Altai Mountain region were found in the years of 2003, 2005, and 2010-2011; in the Khangai Mountain region were found in the years of 2003, 2005, 2007-2008, and 2010-2011; in the eastern steppe region were found in the years of 2001, 2003-2004, and 2007-2010. During the period

2007-2008, larger negative anomalies of snow cover were distributed in northern China.

In April, the snow cover was mainly distributed in the mountain regions, the Altai and Khangai Mountains in Mongolia, and the mountains surrounding the Taklimakan Desert in western China as shown in Fig. 19a. Figure 19b-h and 20a-h show the spatial distribution of anomalies of snow cover April. Snow cover in Mongolia shows the highest value of positive anomalies in 2010. Most regions revealed similar characteristic with that in March, but with low values of the anomalies.

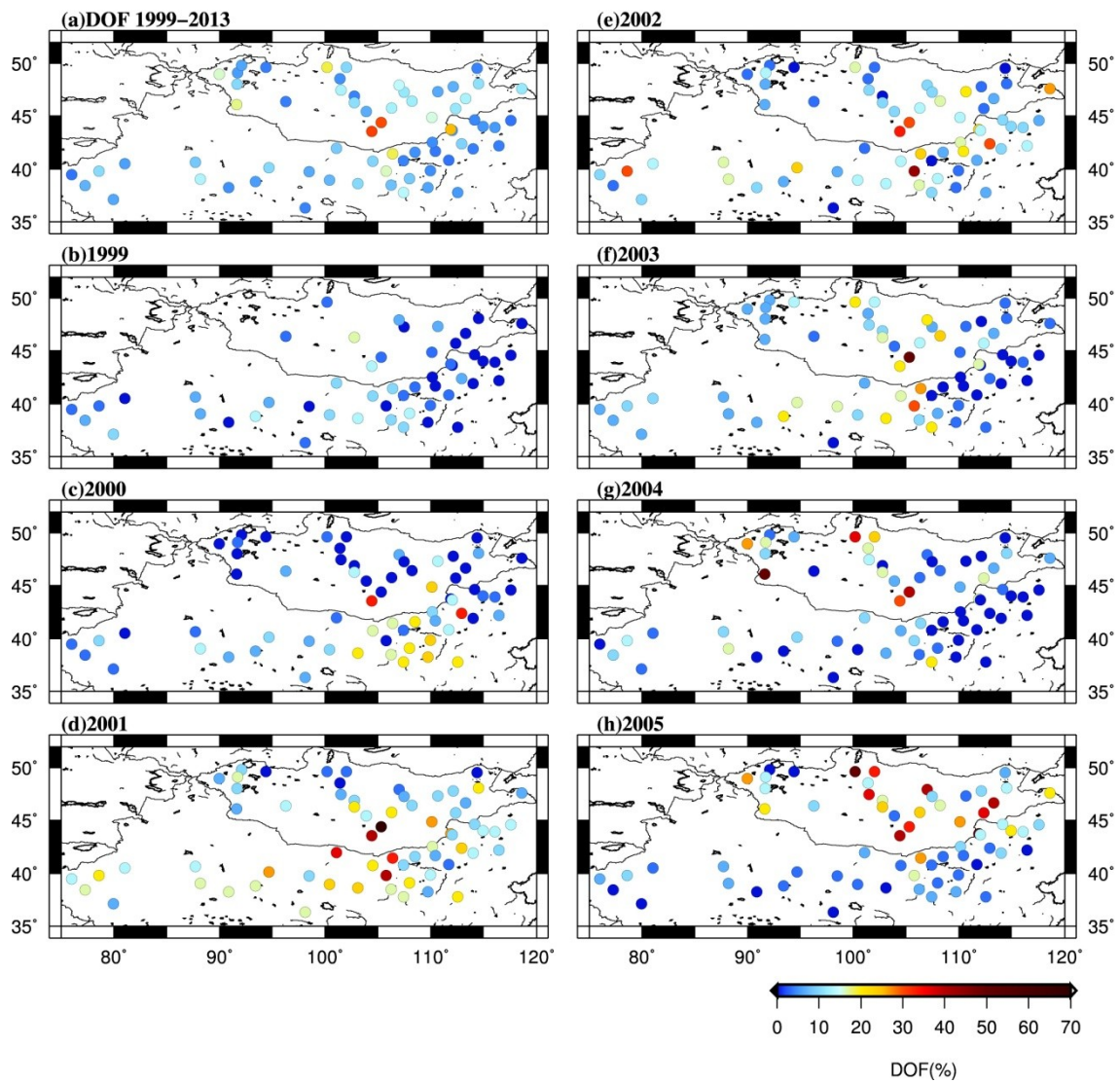


Figure 4. Spatial distributions of the mean DOFs in April for the period of (a) 1999-2013, and for (b) 1999, (c) 2000, (d) 2001, (e) 2002, (f) 2003, (g) 2004, and (h) 2005, respectively.

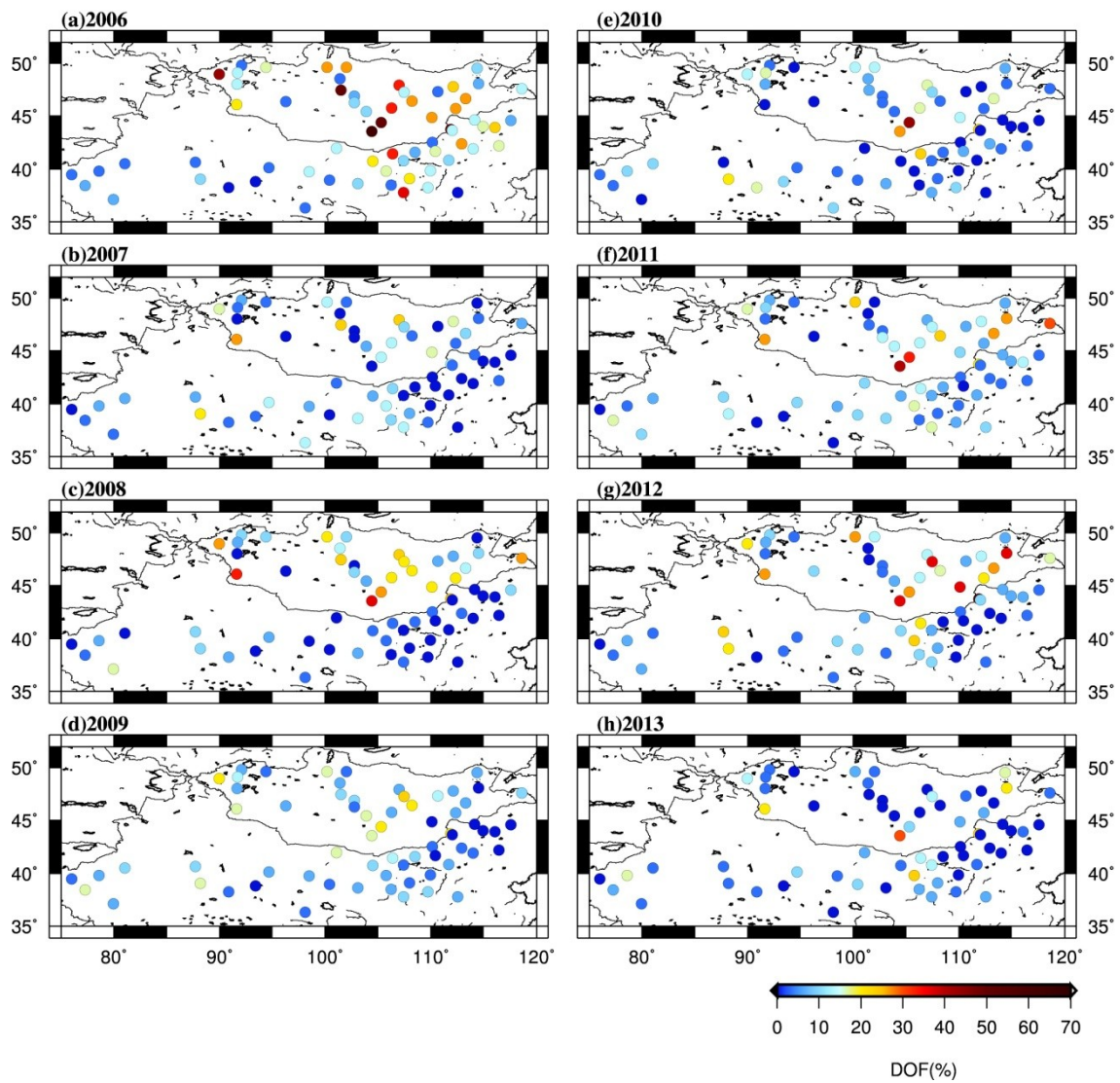


Figure 5. Spatial distributions of the mean DOFs for (a) 2006, (b) 2007, (c) 2008, (d) 2009, (e) 2010, (f) 2011, (g) 2012, and (h) 2013, respectively.

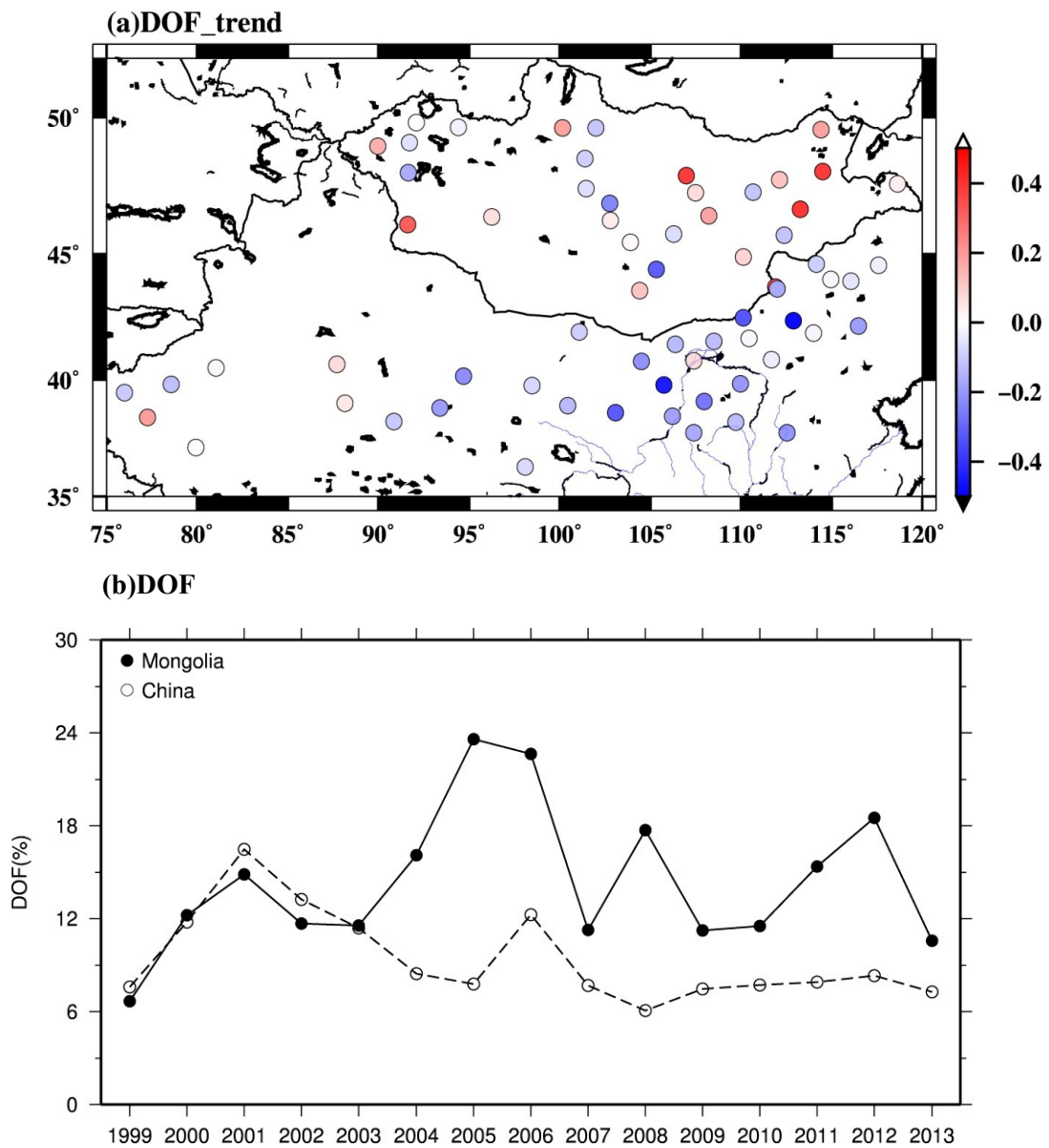


Figure 6. (a) Spatial distribution of the changing trend slope in the mean DOF in April from 1999 to 2103, and (b) inter-annual variations of the average DOF in April of the stations located in Mongolia, and China, respectively, during the period 1999-2013.

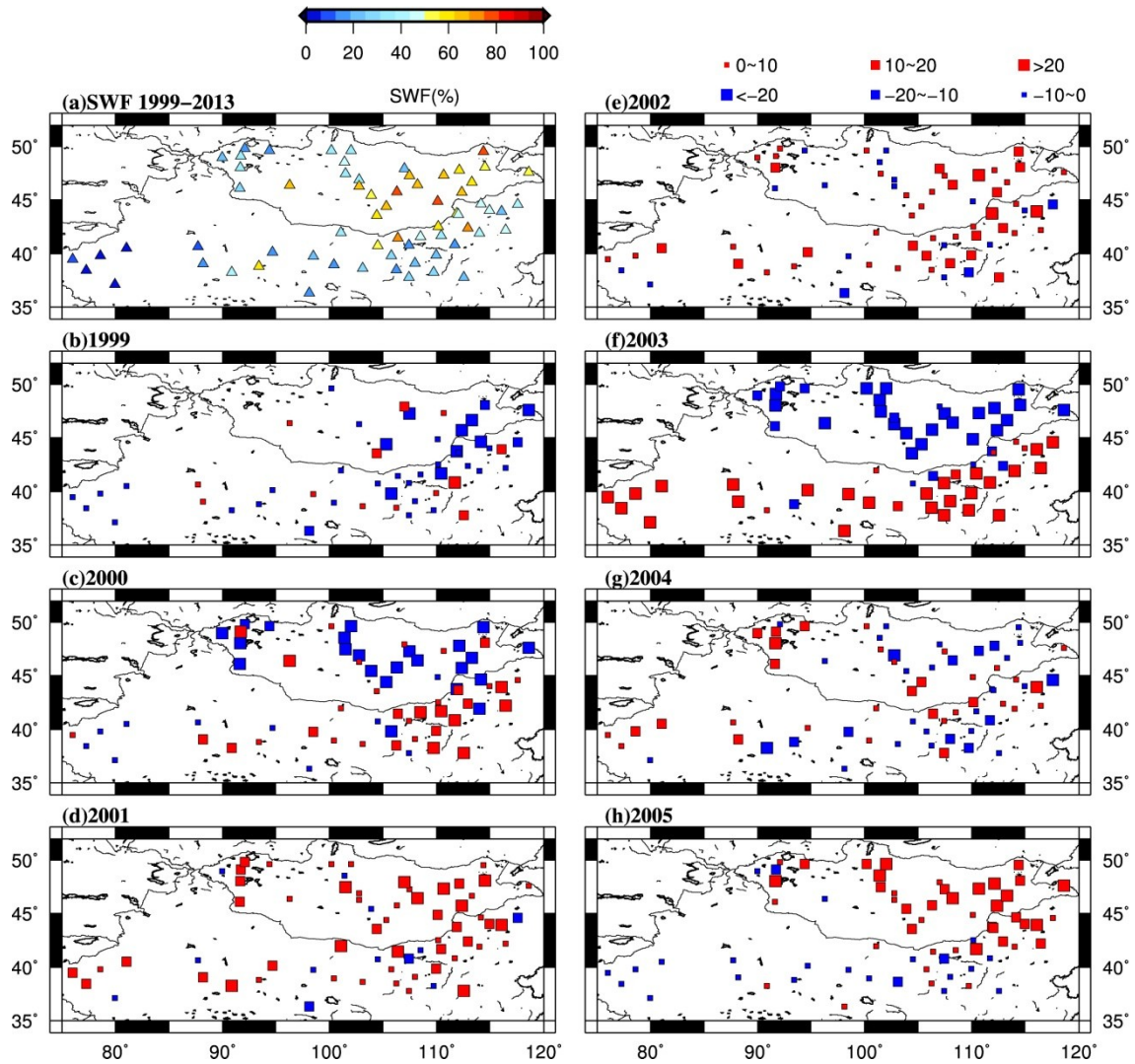


Figure 7. Spatial distributions of (a) the mean SWFs in April during the period 1999-2013, and spatial distributions of anomalies of the SWFs for (b) 1999, (c) 2000, (d) 2001, (e) 2002, (f) 2003, (g) 2004, and (h) 2005, respectively. The red and blue squares indicate positive and negative anomalies, respectively.

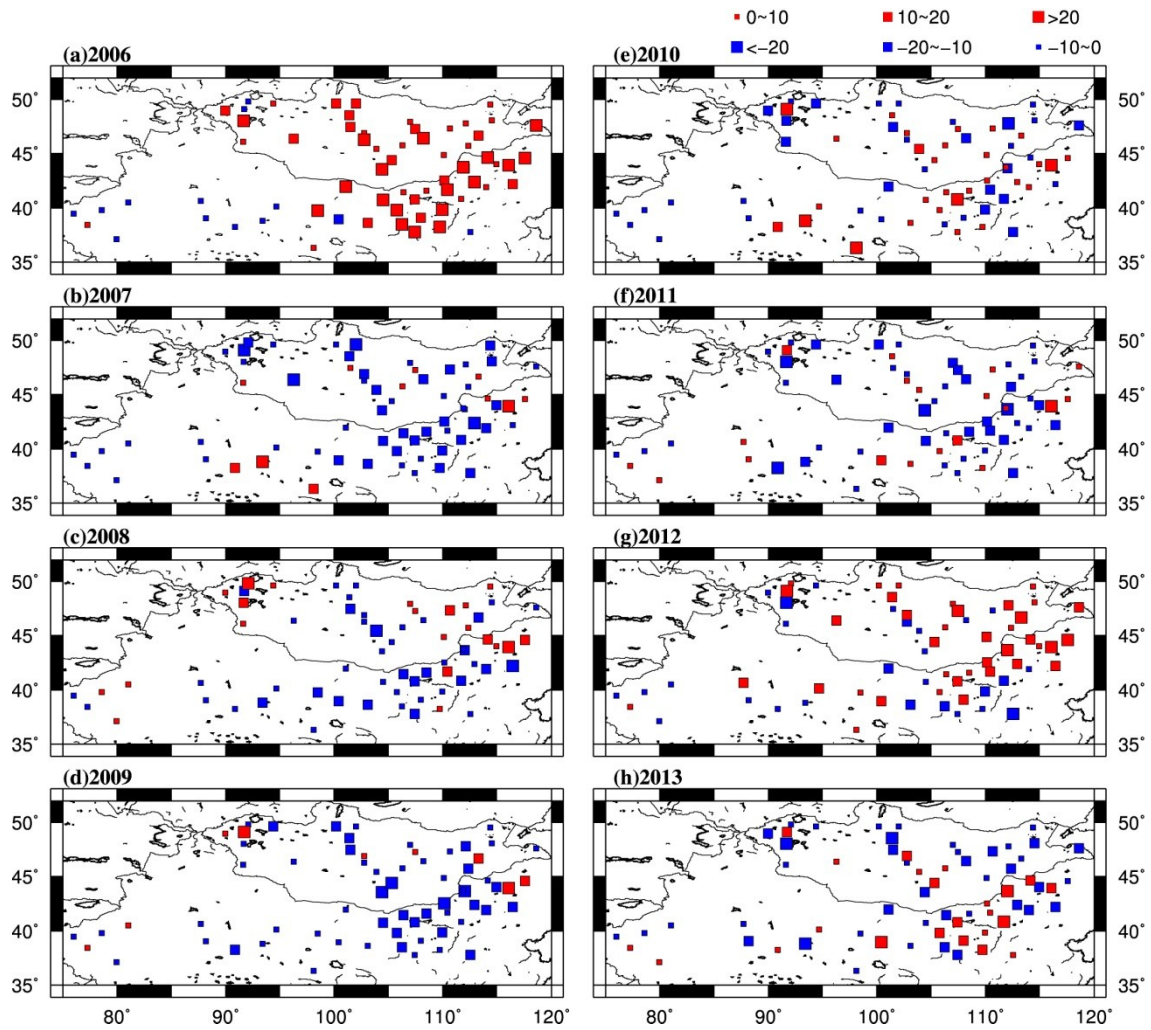


Figure 8. Spatial distributions of anomalies of the SWFS for (a) 2006, (b) 2007, (c) 2008, (d) 2009, (e) 2010, (f) 2011, (g) 2012, and (h) 2013, respectively. The red and blue squares indicate positive and negative anomalies, respectively.

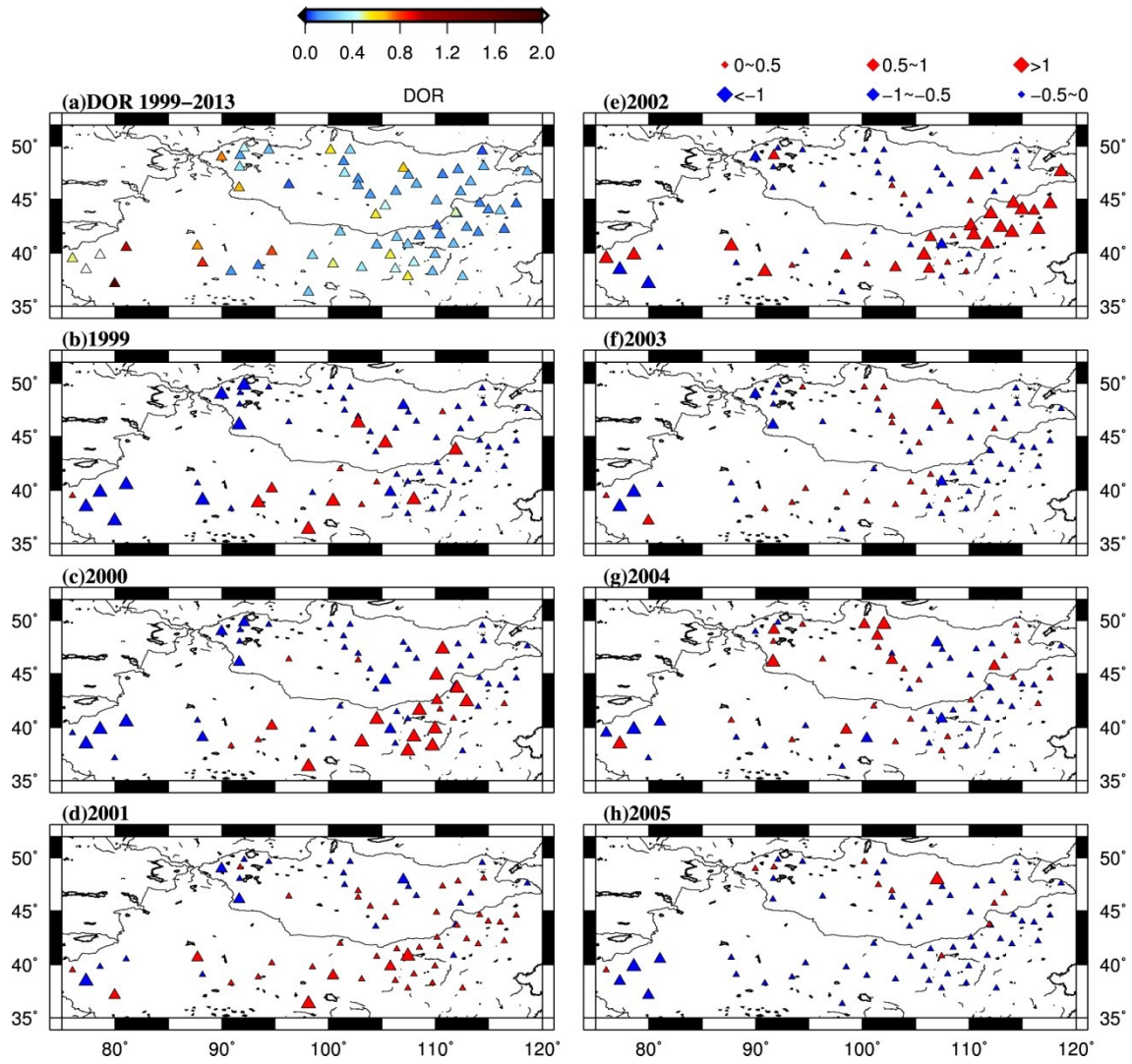


Figure 9. Same as Fig. 7, but for the DOR

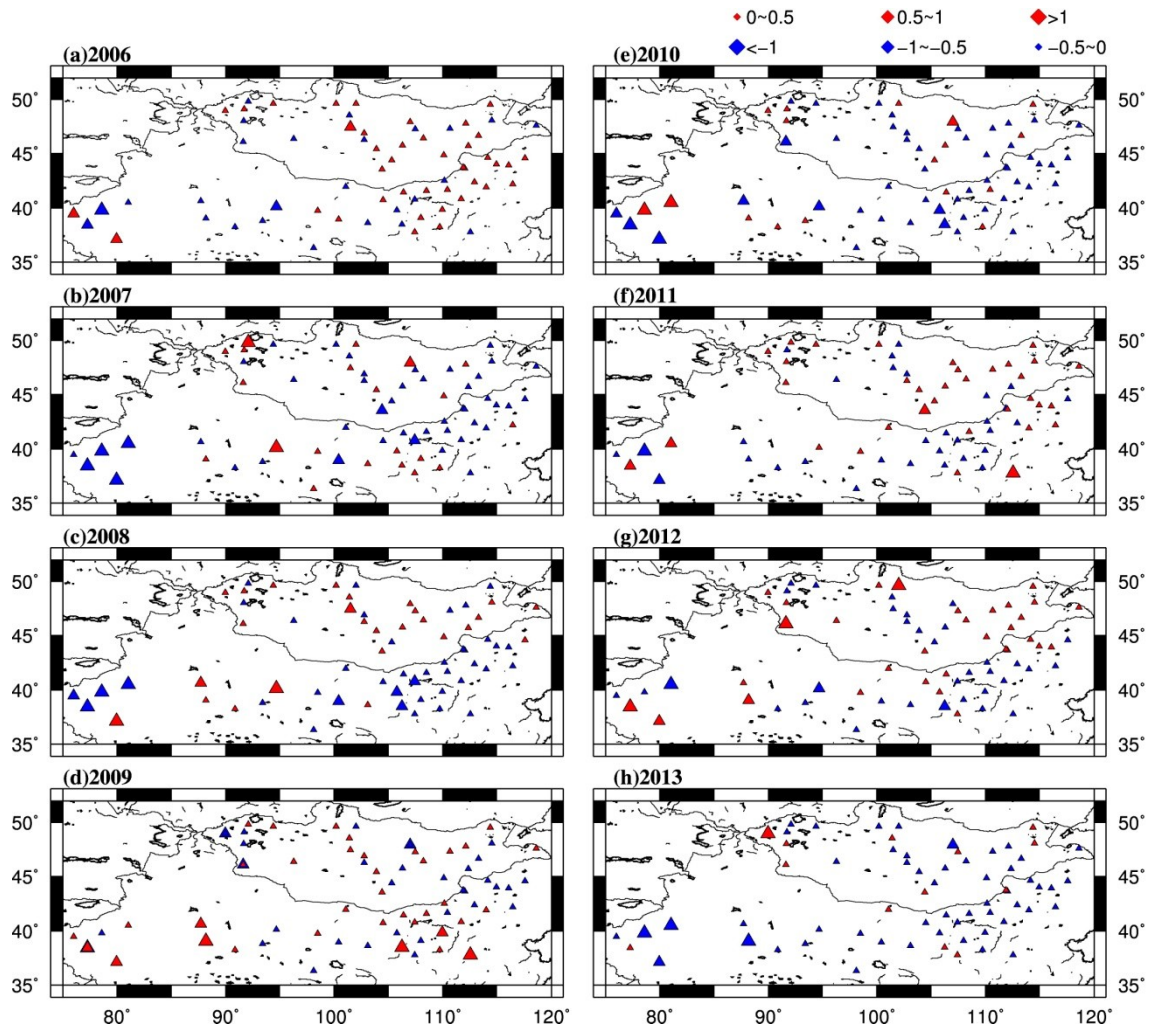


Figure 10. Same as Fig. 8, but for the DOR indicated by triangles.

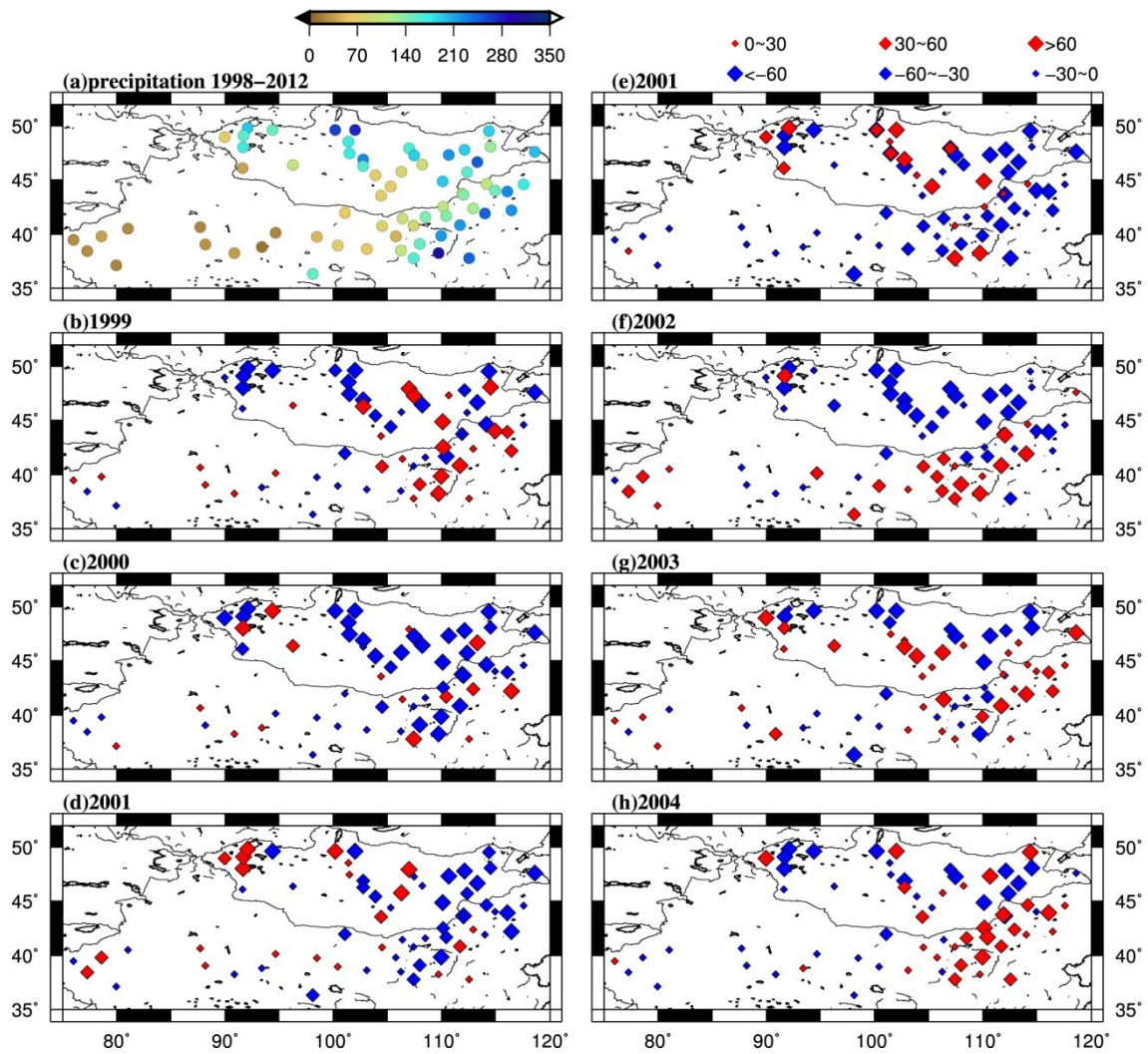


Figure 11. Same as Fig. 7, but for the summer precipitation (June to August) during the period of 1998 to 2012 indicated by diamonds.

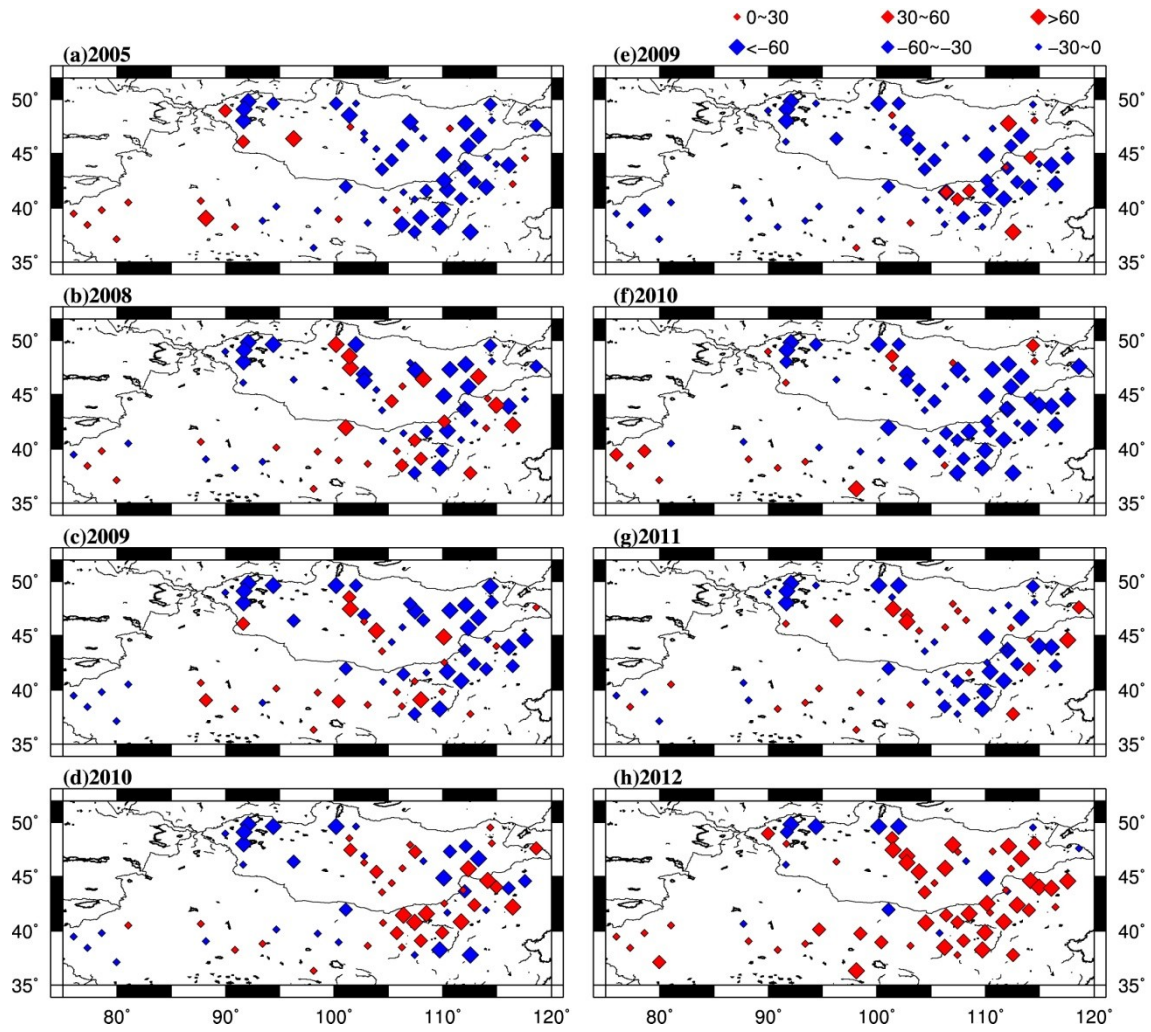


Figure 12. Same as Fig. 8, but for the summer precipitation.

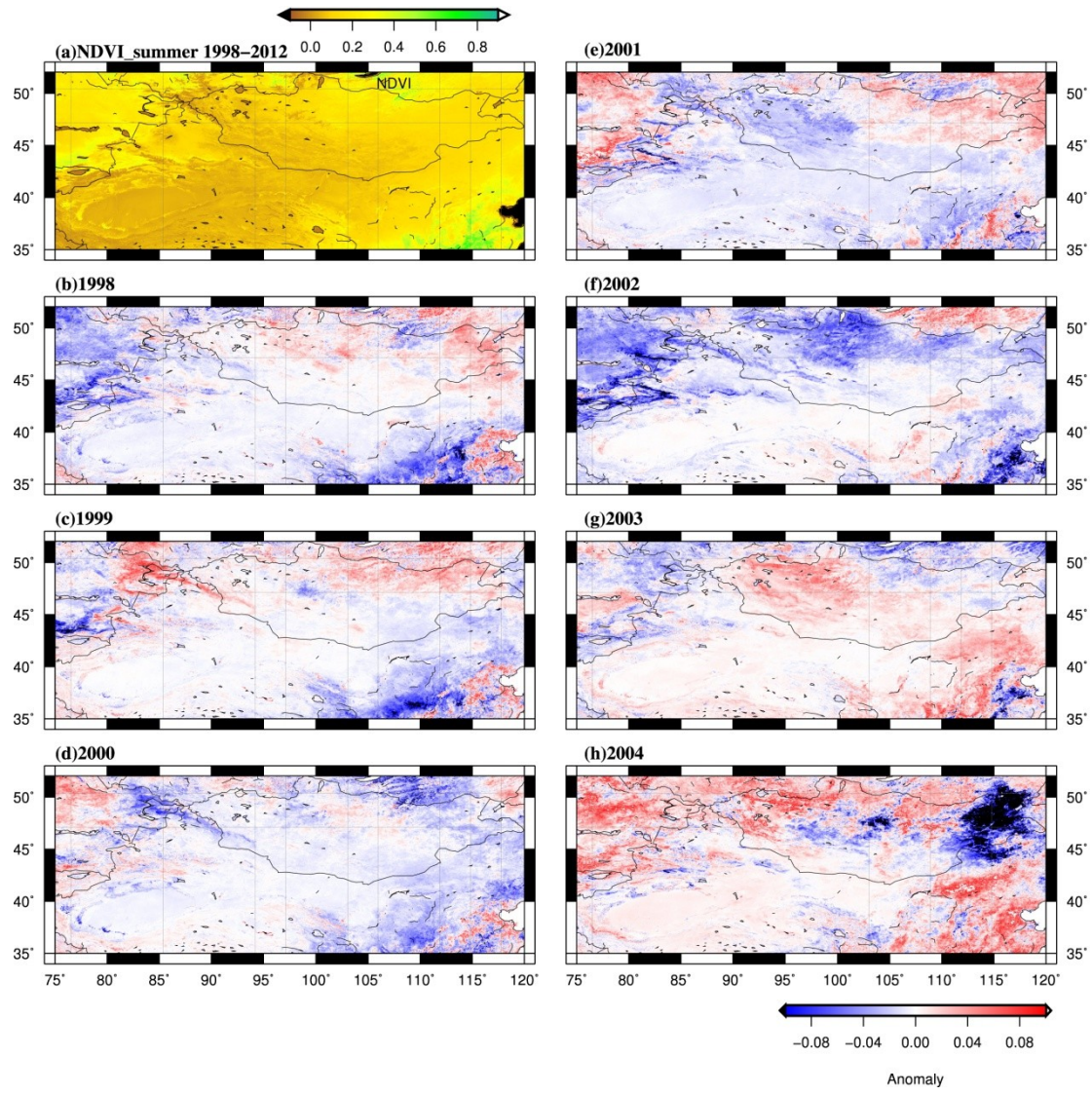


Figure 13. Same as Fig. 7, but for the annual maximum NDVI for the period of 1998 to 2012.

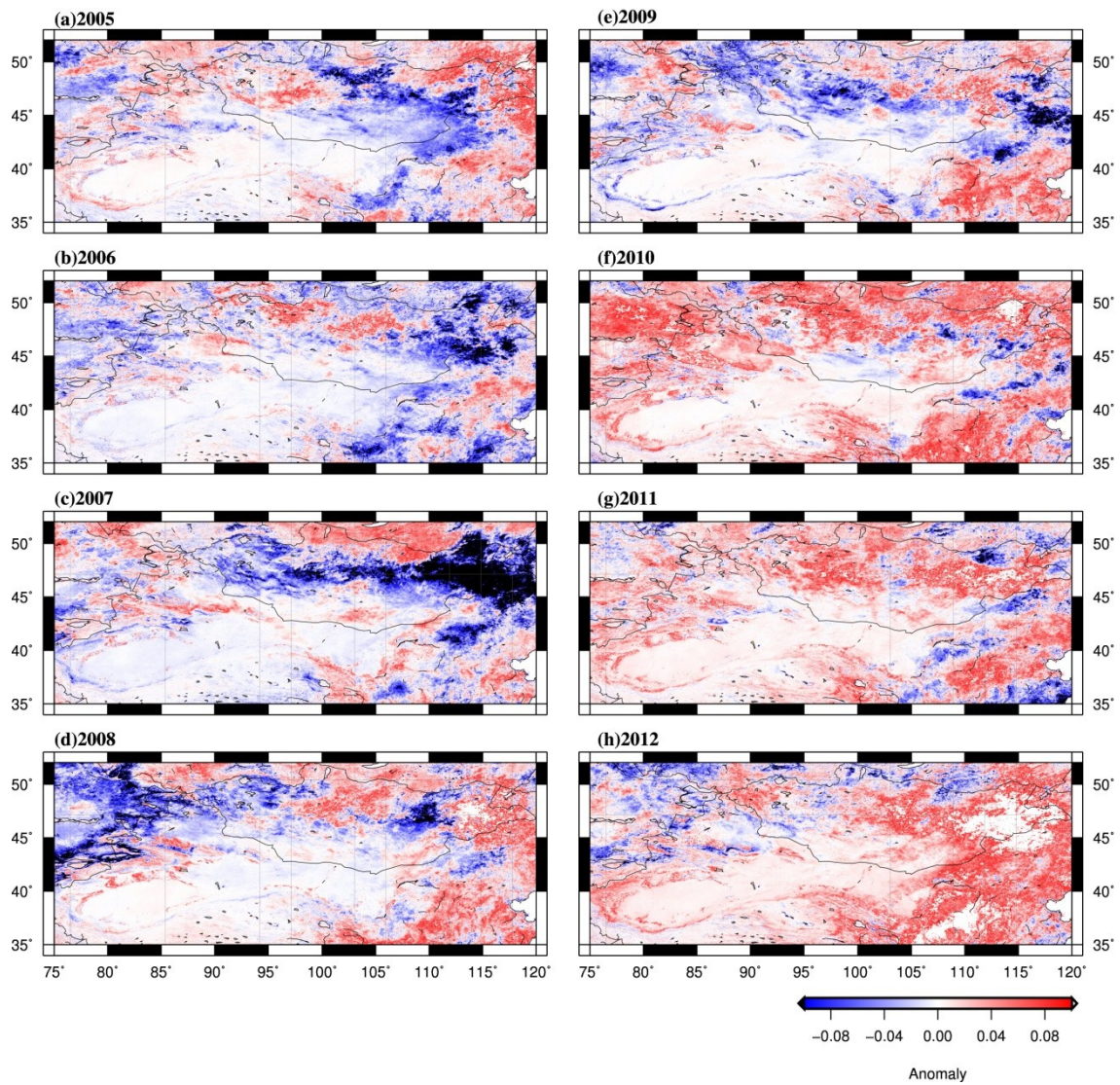


Figure 14. Same as Fig. 8, but for the annual maximum NDVI.

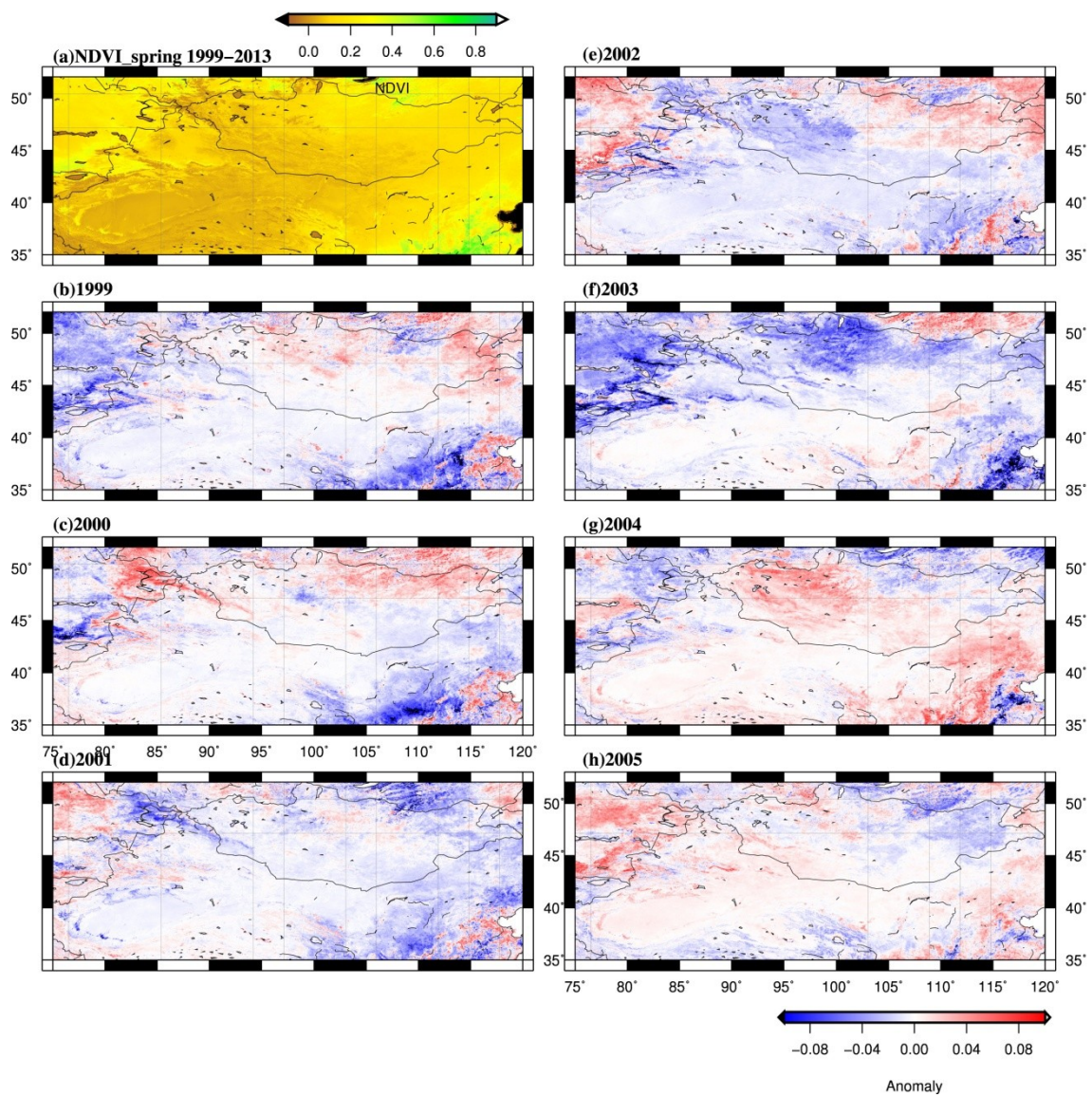


Figure 15. Same as Fig. 7, but for the NDVI in April for the period of 1999 to 2013.

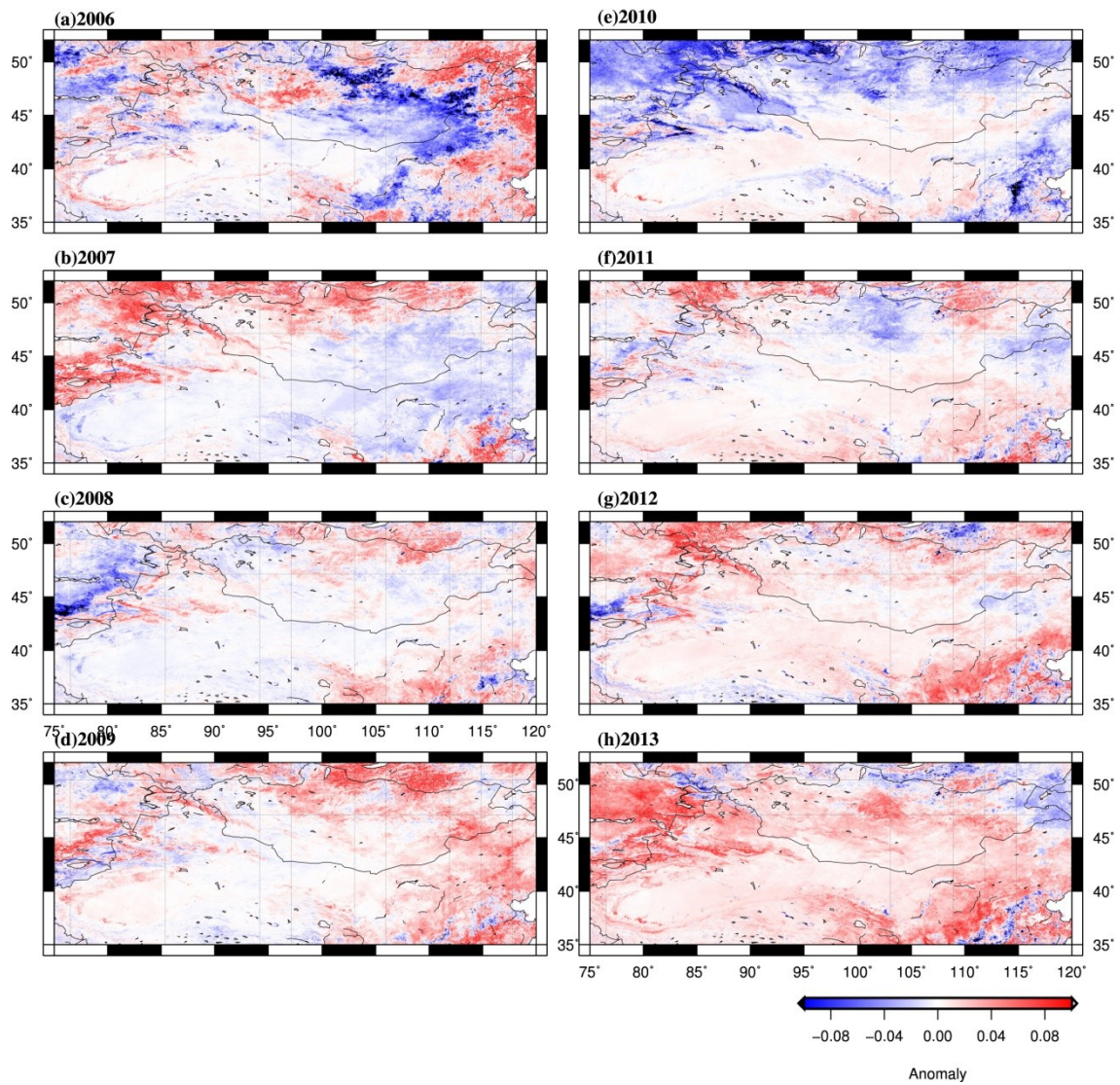


Figure 16. Same as Fig. 8, but for the NDVI in April.

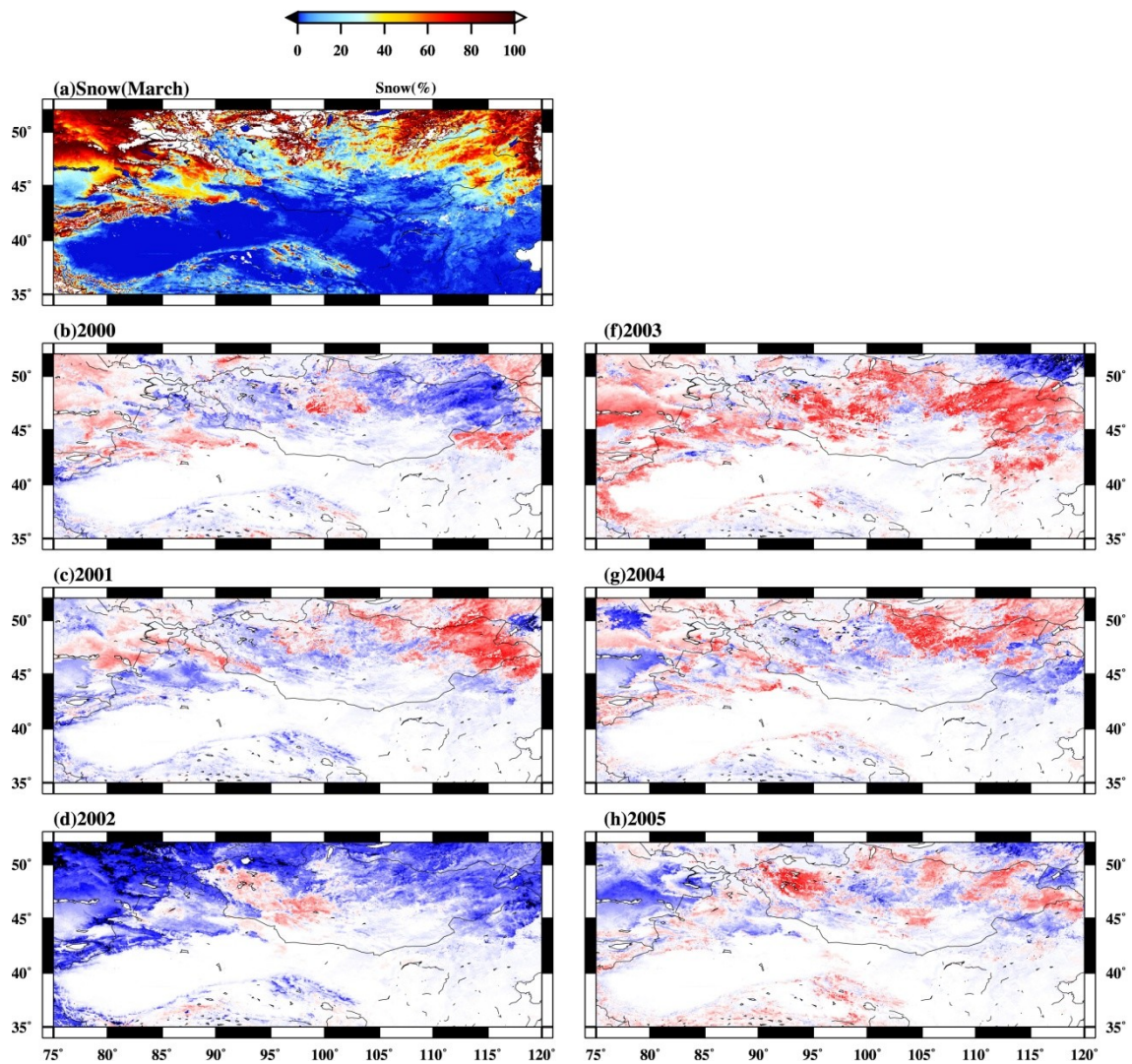


Figure 17. Same as Fig. 7, but for the snow fraction in March for the period of 2000 to 2012.

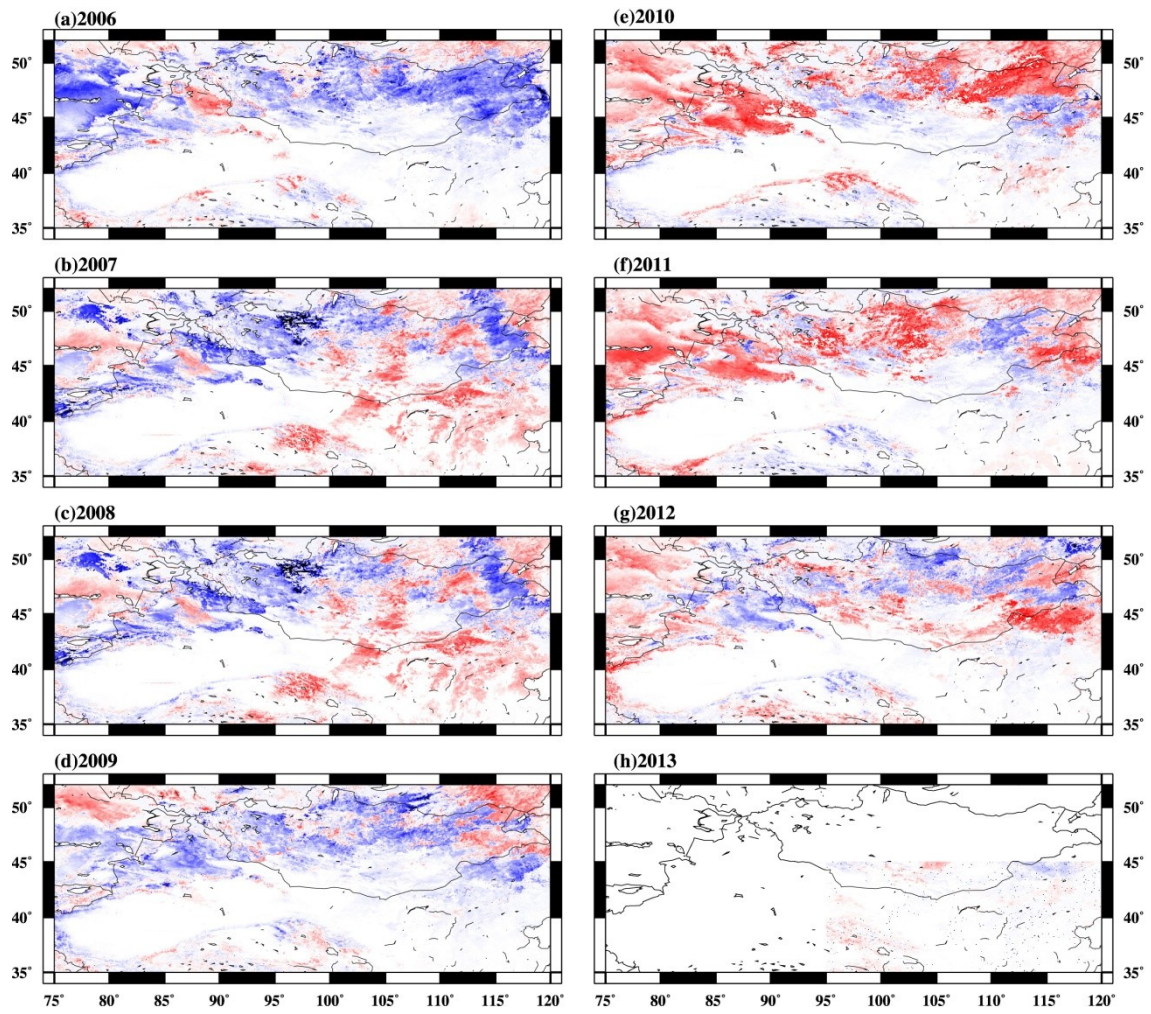


Figure 18. Same as Fig. 8, but for the snow fraction in March.

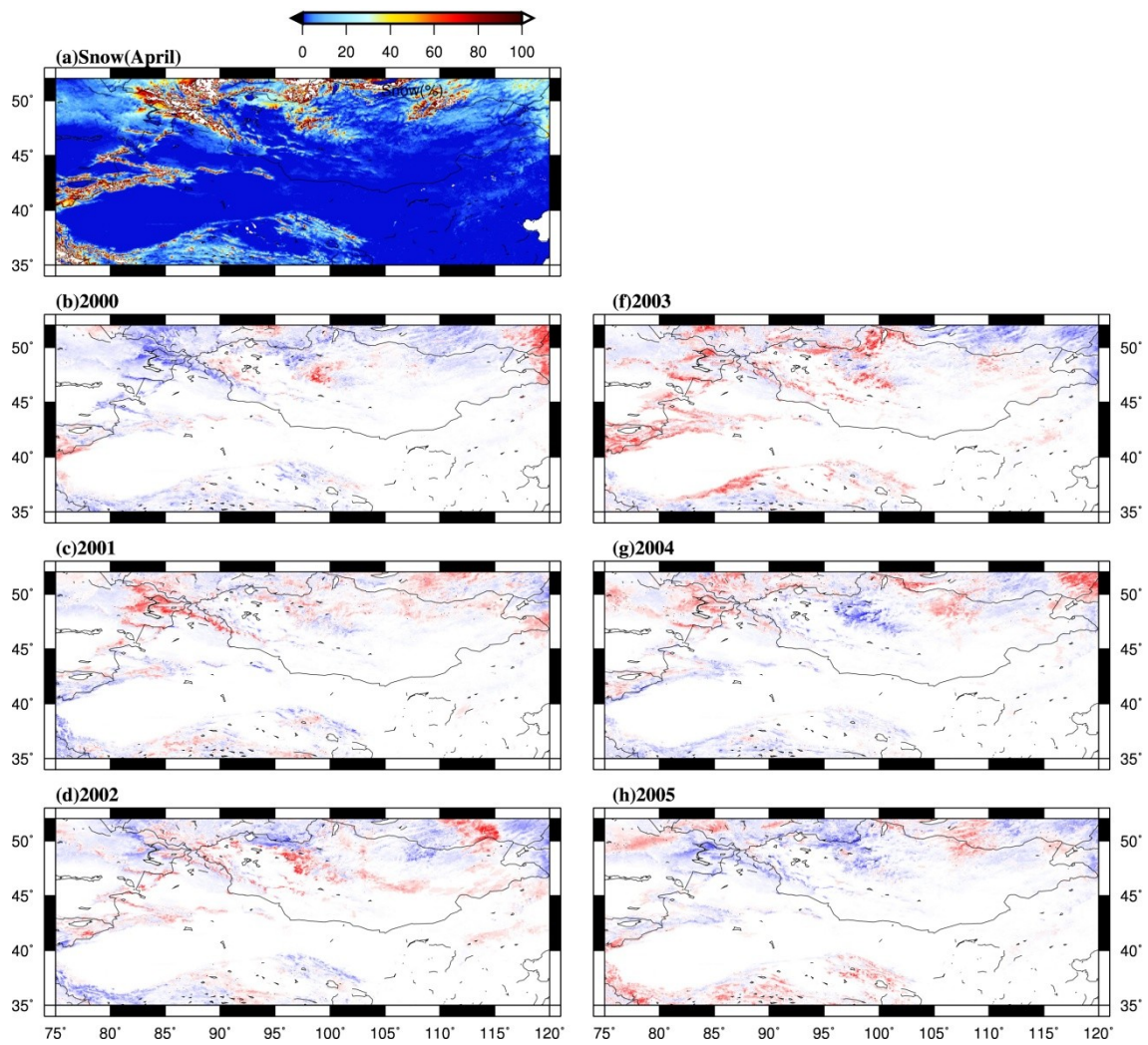


Figure 19. Same as Fig. 7, but for the snow fraction in April for the period of 2000 to 2012.

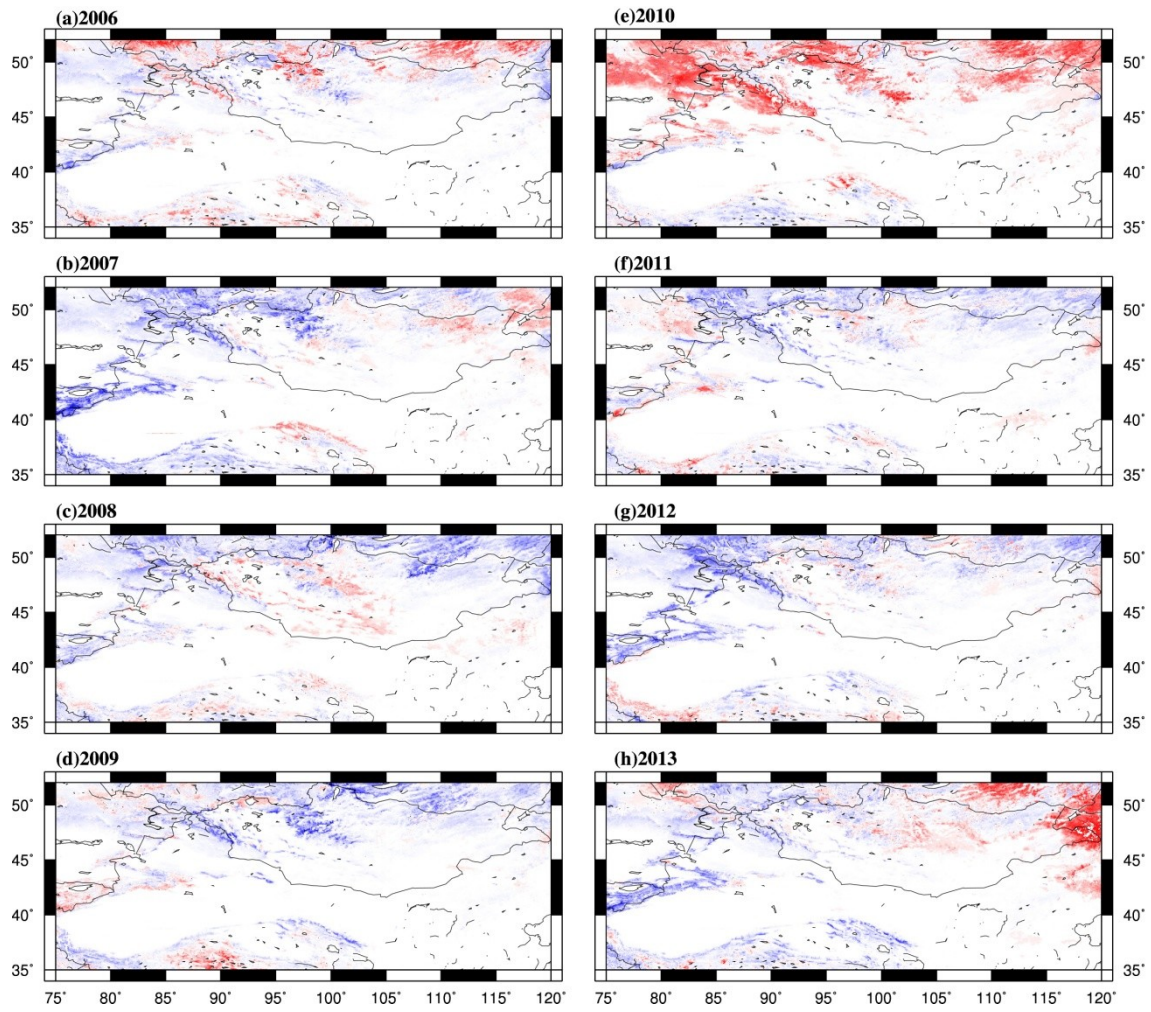


Figure 20. Same as Fig. 8, but for the snow fraction in April.

4. Controlling factor for the recent dust occurrence in East Asia

4.1 Data processing

In order to identify the most significant controlling factor to the inter-annual variations in the DOF, the author classified the stations into five categories in terms of relative contributions of erosivity and erodibility to the inter-annual variations.

The DOF was regressed, on a station basis, on the SWF and the DOR using a linear regression model. If the DOF was significantly related to only the SWF (or DOR) at the 5% significance level ($p < 0.05$), such stations were classified as erosivity (or erodibility) only. If the DOF was significantly related to both the SWF and the DOR, out of the two, a larger value of the correlation coefficient indicates a greater contribution. Such stations were classified as erosivity $>$ (or $<$) erodibility. Regression curves and the correlations between the DOR and the erodibility parameters of the April NDVI (A), annual maximum NDVI (M), summer precipitation (P) and snow cover in March or April (S) were derived at the 5% and 10% significance levels for each station, where the DOF was more strongly related to the DOR.

Figures 21 and 22 show an example of the “erosivity only” at Hovd (91.64°E, 48.02°N) located in the Altai Mountain regions, Mongolia. As illustrated in Fig. 14a, the DOF showed an increasing trend from 2001 to 2005 and then decreased. The variation of SWF shows a similar pattern with the DOF except for the period 2001-2003, with the lowest values of the DOR. Snow cover in March was higher than April, with considerable variations (Fig. 21b). Higher values of summer precipitation and maximum NDVI in the previous year appeared between 2003 and 2005 (Fig. 21c), so did NDVI in the following spring. However, the NDVI was also higher between 2010 and 2012 although the precipitation was less. As shown in Fig. 22, a statistically

significant correlation was found between DOF and SWF ($r^2=0.35$, $p<0.05$), but not found between DOF and DOR ($r^2=0.12$, $p>0.1$).

In the case of Kashi (75.97°E, 39.47°N) located in the Taklimakan Desert, the DOF was high in the period 2000-2002, and then decreased with a decrease in the SWF (Fig. 23). There was almost no snow cover in the spring. Under the arid condition of climate, the precipitation amount in summer is extremely low (< 65mm). However, the vegetation is abundant in summer and the following spring because of a nearby oasis. Figure 24 shows that the DOF was significantly related to both the SWF ($p<0.01$) and the DOR ($p<0.05$) at the 5% significance level. The correlation coefficient in SWF ($r^2=0.53$) is higher than that in DOR ($r^2=0.38$). Therefore, this station is an example of the category “erosivity > erodibility”.

An example of the “erodibility only” station at Naran-bulag (114.14°E, 44.62°N), which is located in the Inner Mongolian steppe is shown in Figs. 25 and 26. Dust outbreaks were not frequently observed with relatively high values of the SWF. The DOF were higher when the vegetation cover was less, such as in the years of 2005-2006. In the dusty years, the spring snow cover was also less. As shown in Fig. 26, the correlation between DOF and DOR is statistically significant ($r^2=0.96$, $p<0.00001$). Regression curves and correlations in nonlinear regression between DOR and erodibility parameters of A, M, P and S show that the most contributing factor was A ($r^2=0.46$, $p<0.1$).

Figure 27 shows time series of the DOF, SWF, DOR and A, M, P and S at Choir (108.21°E, 46.45°N), Mongolia. The DOF increased with the DOR between 2000 and 2013. The SWF varied considerably from year to year before 2006, and it showed a peak value in 2005, resulting in the highest DOF. The NDVI was in a range of 0.1-0.15

in April and of 0.2-0.4 in summer. Snow cover was larger in March than in April. The total amount of summer precipitation was about 100 mm except for 2006 with a high value of 383 mm. Figure 28 illustrates the results of that the DOF at Choir was related to the combined impact of erosivity and erodibility, while the contribution of the DOR ($r^2=0.86$, $p<0.00001$) was greater than that of the SWF ($r^2=0.30$, $p=0.05$). This station is in the category of “erosivity < erodibility”. As for the erodibility parameters, the most significant factor was M ($r^2=0.35$, $p<0.05$).

4.2 Controlling factors

The purpose of the present study is to identify the most significant controlling factor to the DOF, and the author classified the stations into five categories in terms of relative contributions of the controlling factors: erosivity only, erosivity > erodibility, erodibility > erosivity, erodibility only, and unclassified. Those stations with the identified controlling factor revealed regional characteristics. A map of the spatial patterns of factors that had a controlling impact on dust occurrence is shown in Fig. 29.

4.2.1 Desert and desert-steppe region

Strong wind shows significantly positive correlations with dust outbreaks at most stations in the Taklimakan Desert, west of the Hexi Corridor (Dunhuang, 94.67°E, 40.15°N), and on the south side of the Altai Mountain region (desert-steppe). Thus, erosivity is the driving force to cause dust outbreaks. The DOF at those stations was less than 10%, resulting from infrequent strong winds with lower SWF values (figure not shown) of < 5% and 5-10% in the Taklimakan Desert and the Altai Mountain region, respectively. The DOF at the other stations was higher than 10%, resulting from higher values of the DOR.

4.2.2 Steppe region

Erodibility, rather than erosivity, has a significant impact on dust occurrence in the Mongolian and Inner Mongolian steppes. In the Mongolian steppe, the summer precipitation or the annual maximum NVDI in the previous year is responsible for the year-to-year variations in the DOF. The connection between summer precipitation and the DOF in the following spring is bridged by soil moisture. The soil moisture anomaly, which depends on summer precipitation, is considered to act as a maintained memory through the freezing winter months to the spring, as reported by Shinoda and Nandintsetseg (2011). When the temperature decreases below 0°C, the soil water anomaly is preserved by soil freezing. In the following April, the frozen soil melts as the temperature increases, providing a wet land surface condition that suppresses the dust outbreaks. As for the annual maximum NDVI, Kurosaki et al. (2011b) proposed a dead-leaf hypothesis for the Mongolian grasslands, which has been modeled by Nandintsetseg and Shinoda (2015). In this hypothesis, the summer vegetation anomaly, which depends on precipitation and soil moisture, remains into the next spring due to the coverage of dead leaves on the top of the soil moisture. The dead leaves decrease erodibility and reduce the occurrence of dust outbreaks.

On the other hand, an increasing trend in the spring NDVI reduces the occurrence of dust outbreaks in the Inner Mongolia steppe. The Chinese government's policy of deferring spring grazing in Inner Mongolia increased the spring vegetation cover and the grassland productivity (e.g., Ma et al., 2014), leading to low DOF values. Playing a similar role to the vegetation, the spring snow cover also reduces the DOF by suppressing wind erosion.

One exception seen is at Xilin-hot (116.06 °E, 43.95 °N), where the DOF was controlled by erosivity. The reason for this exception is unclear.

4.2.3 Loess Plateau

In the desertified areas in the Loess Plateau, the occurrence of dust outbreaks is primarily controlled by the SWF or M. The stations, Otogo-qi (107.97 °E, 39.1 °N), Yulin (109.69°E, 38.23°N), and Jartai (105.74°E, 39.78°N), are located in the region where aeolian desertification exhibited a reversing trend (that is, likely with restored vegetation), as illustrated by the map of Wang et al. (2008) (Fig. 30). Although the map indicates the condition of desertification in 2000, the trend in the annual maximum NDVI from 2000 to 2012 (see Fig. 31) at the stations around the Loess Plateau was less than 1%. Thus, the author considers that the condition of desertification is similar to that for the current decade. The annual maximum vegetation observed in the summer appeared to suppress dust outbreaks in the following spring at these stations. Spring vegetation expressed by NDVI in April also had a negative impact on dust outbreaks at Yulin. The natural vegetation at Yulin was from the southeast forest grassland to the northwest grassland (Wang et al., 2012). As one of the key regions of the Three-North Shelter Program, which was initiated in 1978 and was planned to be completed the project's goal around 2050, it has been suggested that the afforestation also increased the vegetation cover at Yulin (e.g., Liu et al., 2013).

In contrast, the other two stations, Yanchi (107.39°E, 37.78°N) and Dongsheng (109.97°E 39.83°N), are located in the desertified (not reclaimed) areas in the map of Wang et al. (2008). The DOF at these two stations was controlled by erosivity.

Since the DOR might be controlled by multiple erodibility parameters, the

significant factor was not identified at some stations by the simple linear regression analysis in the present analysis.

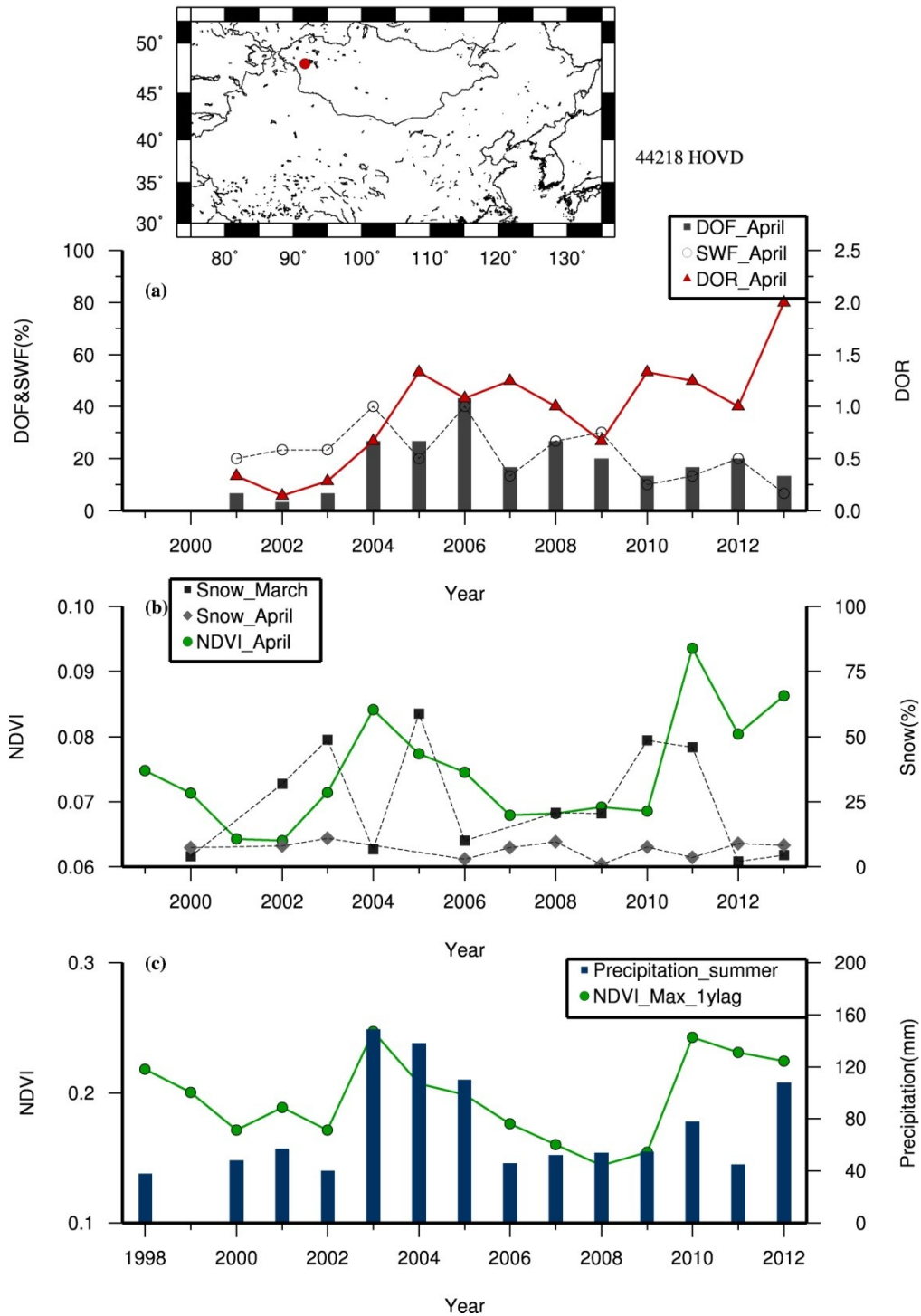


Figure 21. Inter-annual variations of (a) DOF, SWF, DOR in April, (b) NDVI in April and snow coverage in March and April during the period 1999-2013 and (c) summer precipitation (June to August) and annual maximum NDVI during the period 1998-2012 at Hovd, Mongolia.

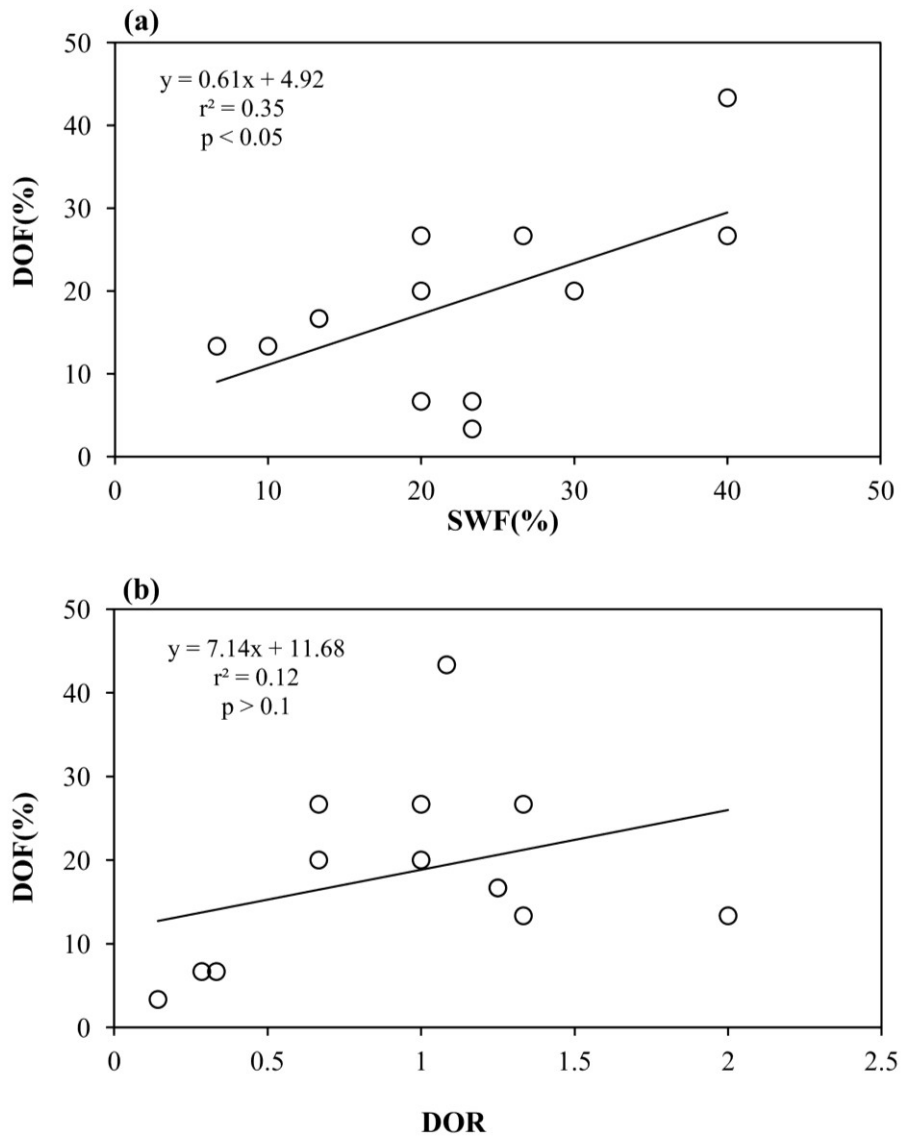


Figure 22. Correlations between DOF and (a) SWF, and (b) DOR in April 1999-2013 at Hovd.

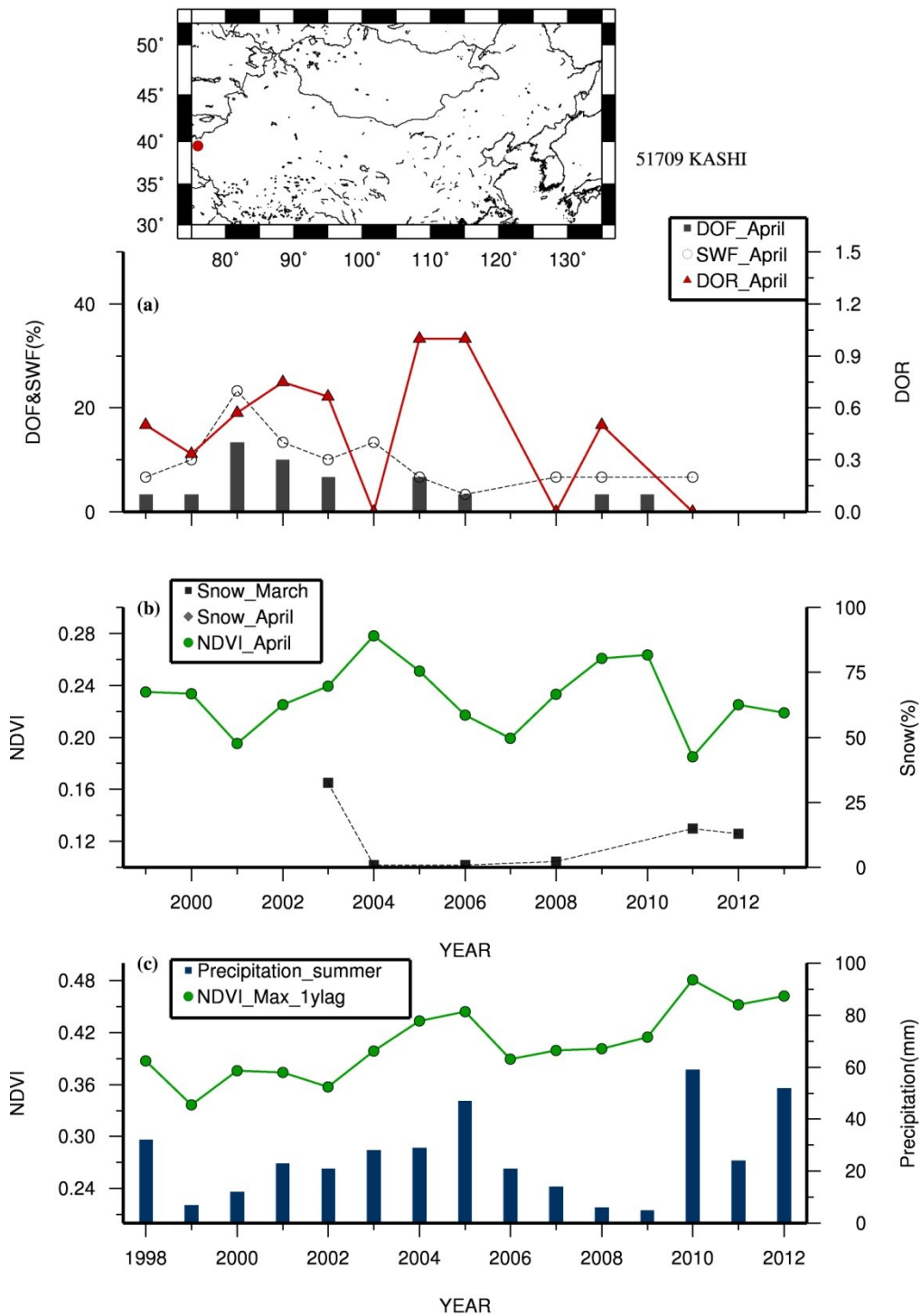


Figure 23. Same as Fig. 21 except for the station Kashi, Xinjiang.

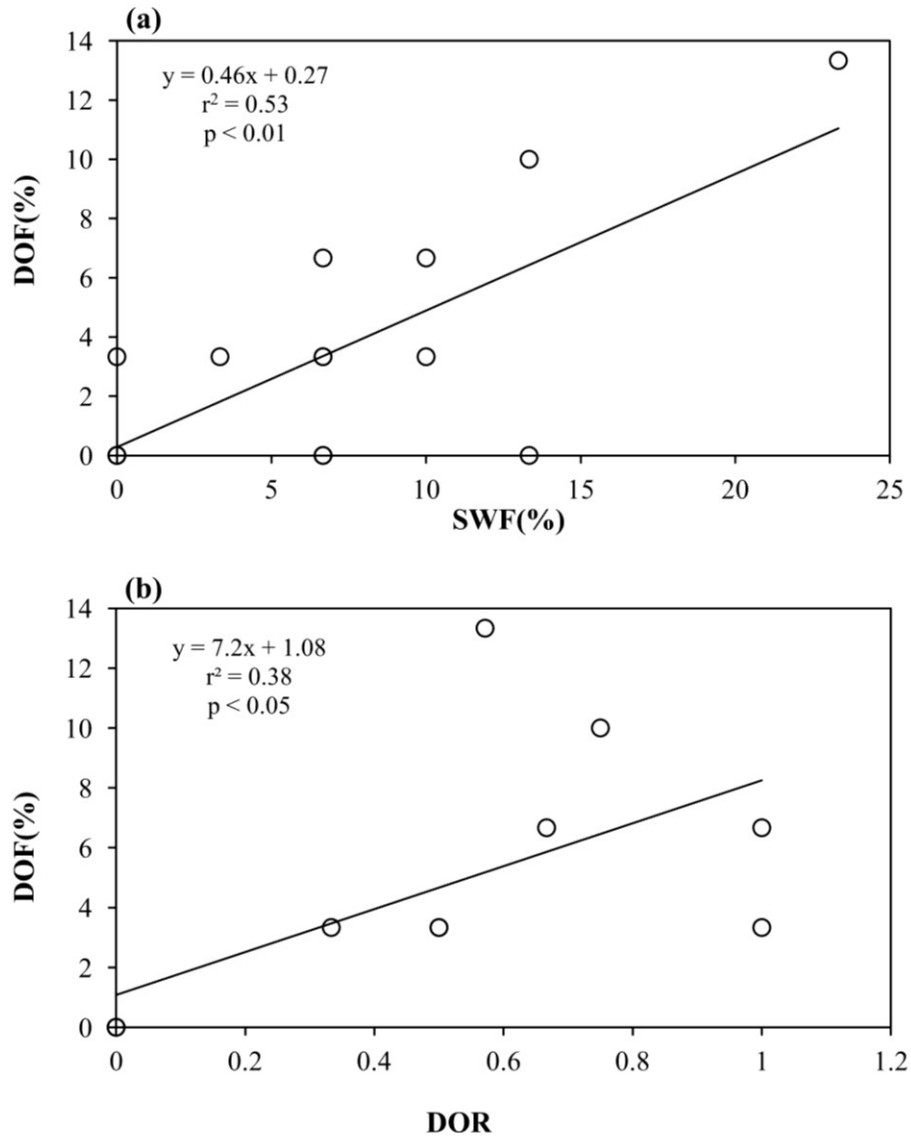


Figure 24. Same as Fig. 22 except for the station Kashi, Xinjiang.

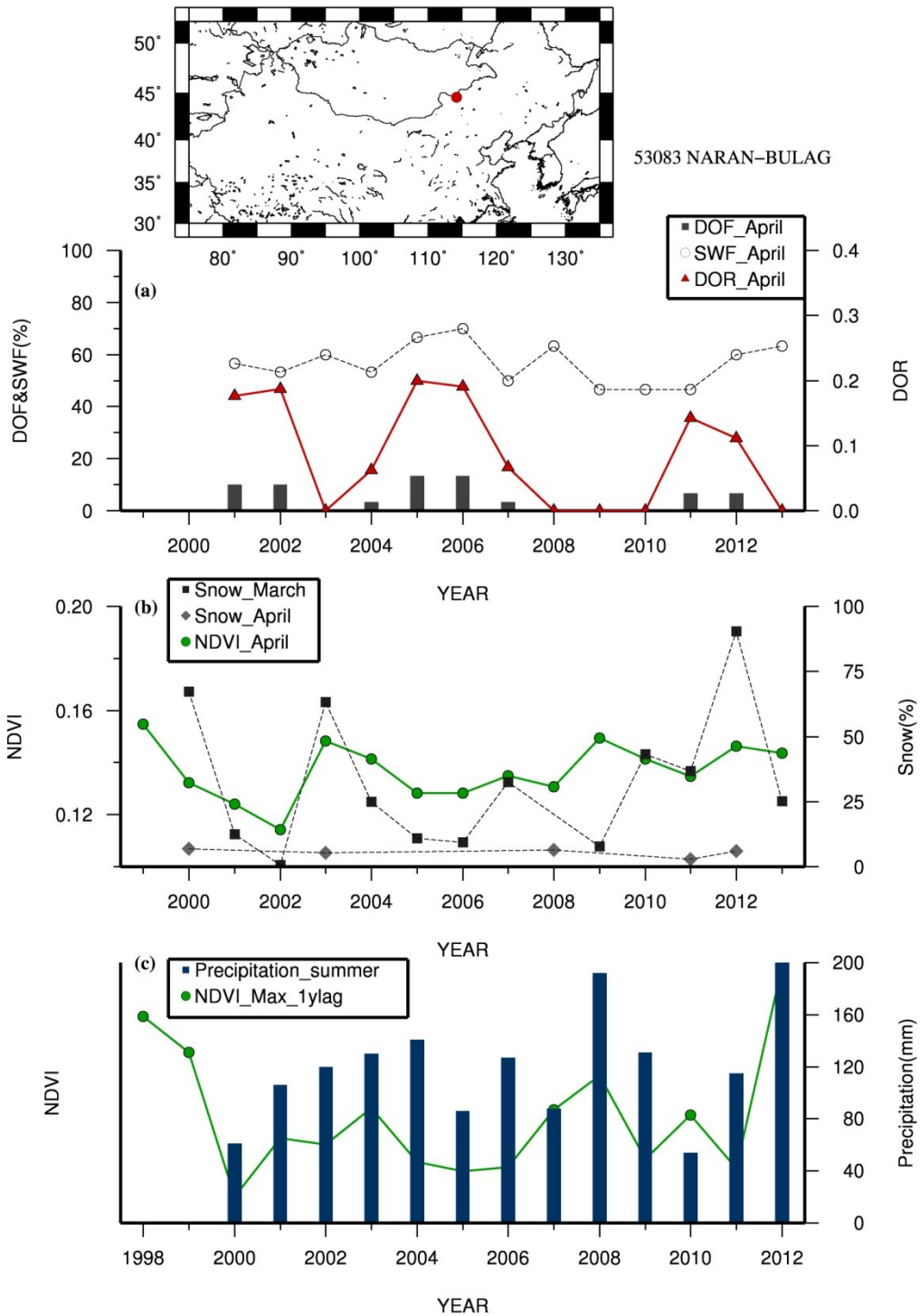


Figure 25. Same as Fig. 21 except for the station Naran-bulag, Inner Mongolia.

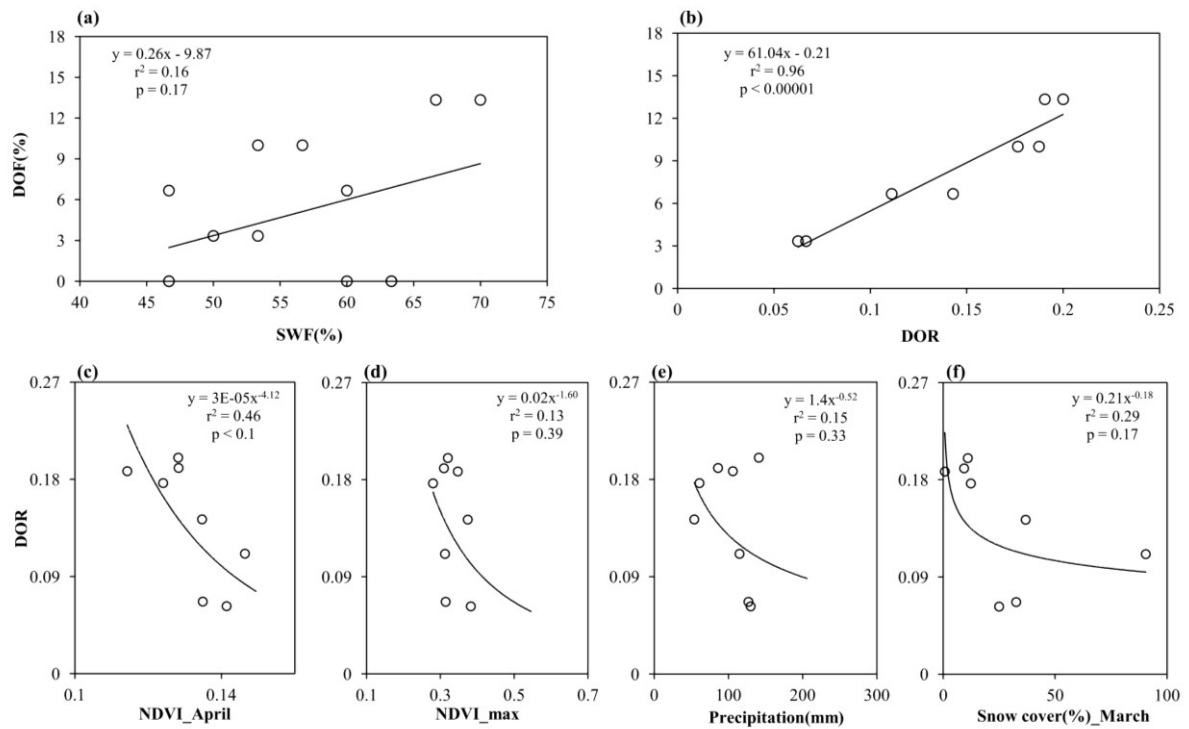


Figure 26. Scatter diagrams for (a) DOF and SWE, (b) DOF and DOR in April 1999-2013; DOR and (c) NDVI in April, (d) annual maximum NDVI and (e) summer precipitation (June to August) in the previous year, and (f) snow cover in March at Naran-bulag, Inner Mongolia.

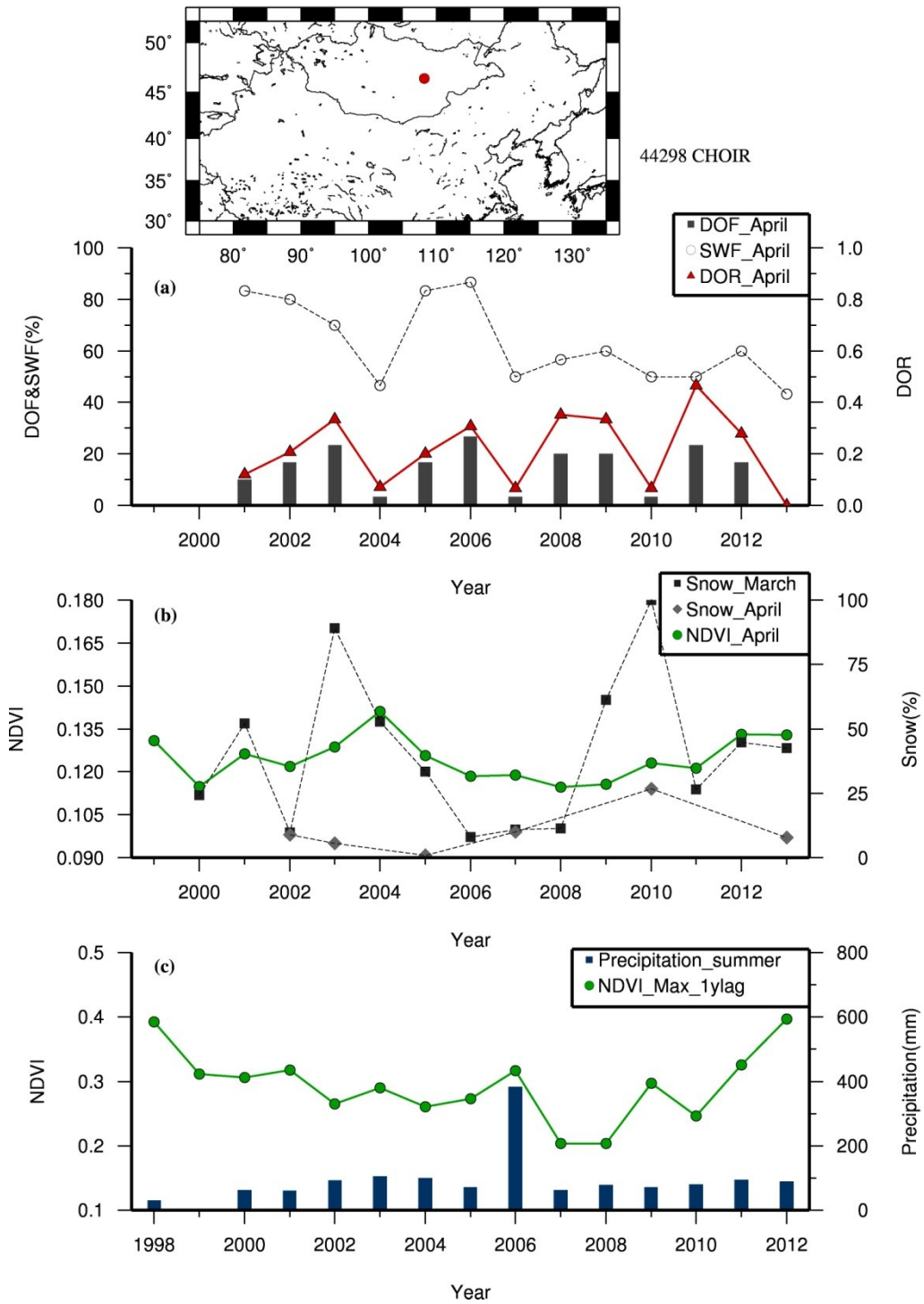


Figure 27. Same as Fig. 21 except for the station Choir, Mongolia.

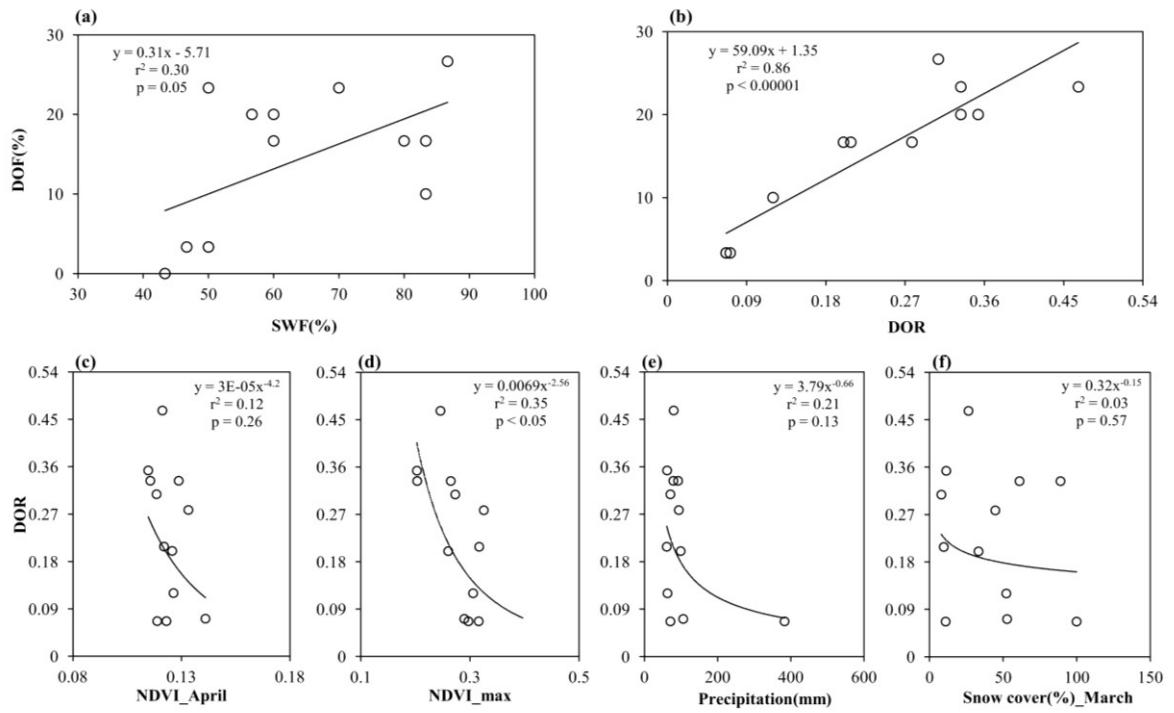


Figure 28. Same as Fig. 26 except for the station for the station Choir, Mongolia.

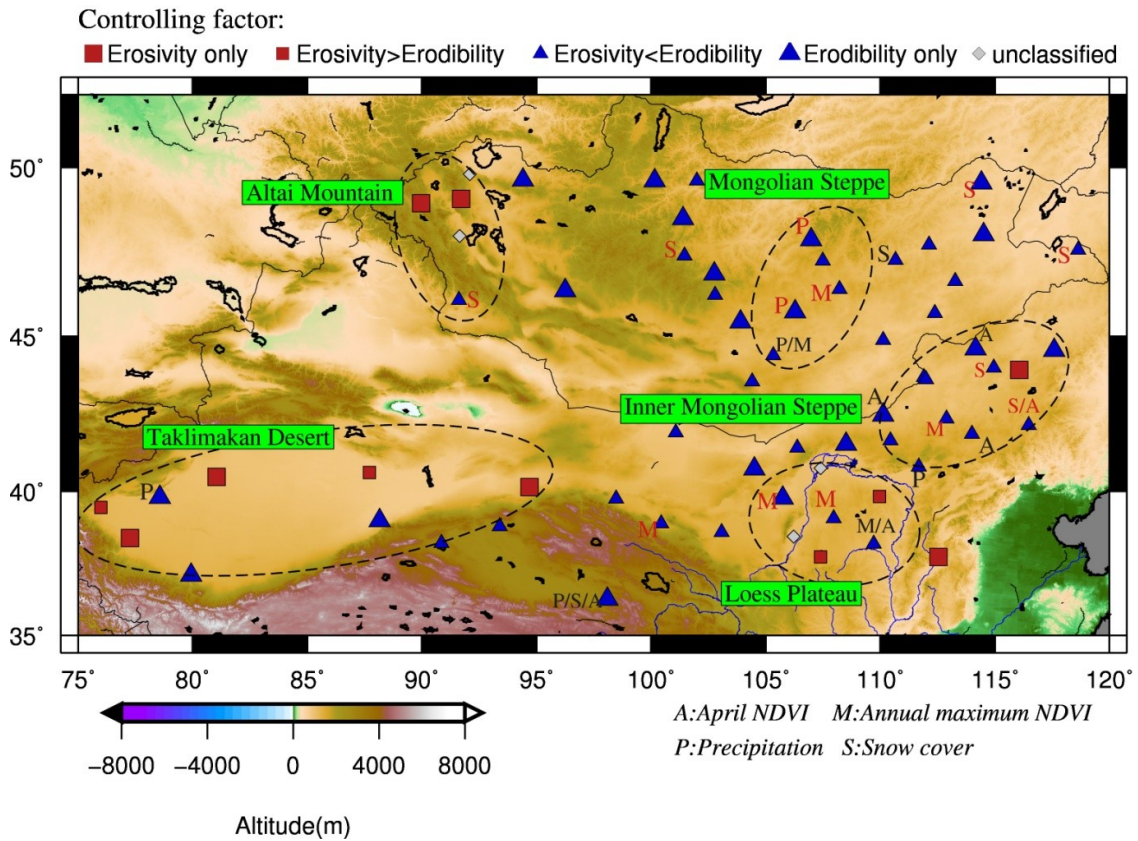


Figure 29. Map of the controlling factors for dust emission in East Asia. The stations, where erosivity shows statistically significant correlation with the DOF at 5% confidence level are shown in red squares. The stations, where erodibility shows a stronger correlation with the DOF are shown in blue triangles. The stations, where spring snow cover, spring NDVI, annual maximum NDVI and precipitation in the previous summer controls DOR, are shown by “S”, “A”, “M”, or “P”, respectively at 5% (red) and 10% (black) confidence level. Background color illustrates altitude

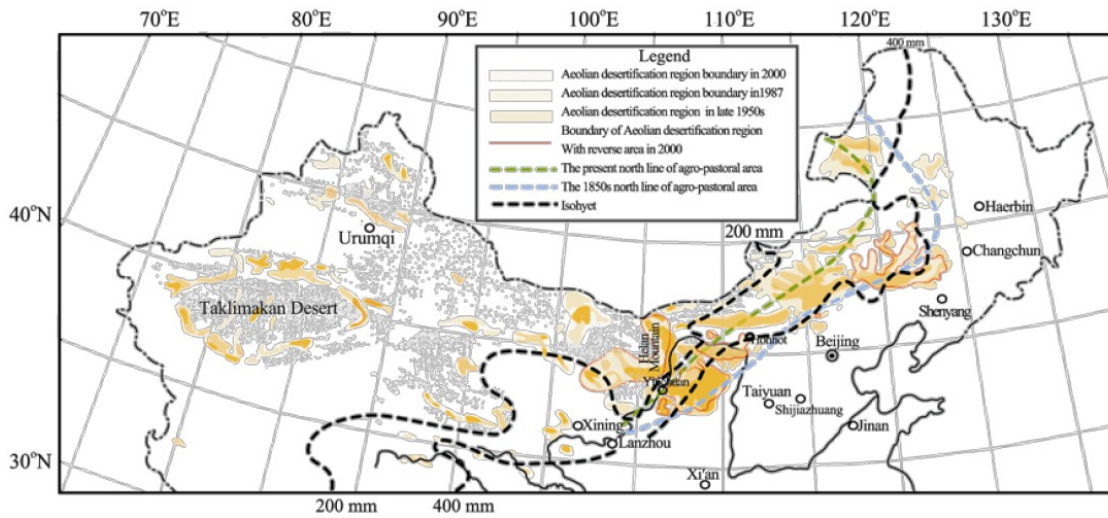


Figure 30. Spatial distributions of aeolian desertified land in Northern China in 1950s, 1987, and 2000. Due to restoration policy, the desertification was reversed in some areas in the Northern China by the end of 1990s. Human activities have also pushed the agro-pastoral boundary northwards by approximately 200 km from 1950s to 2000 (Wang et al., 2008a).

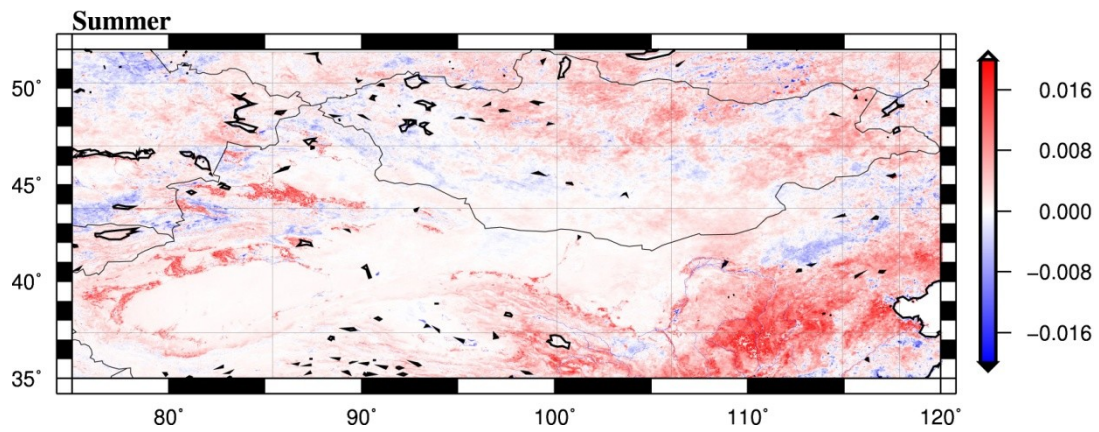


Figure 31. Spatial distributions of the changing trend slope in summer NDVI from 1998-2012. An increasing (decreasing) trend is presented by red (blue) color in background.

5. Discussion

5.1 Dust source regions

Sun et al. (2001) studied the dust storms over the 40 years between 1960 and 1999 and indicated that the major dust source was the Gobi Desert in Mongolia and northern China, and another dust source was the Taklimakan Desert. The Taklimakan Desert and the Gobi Desert in Inner Mongolia were also suggested as two major sources of dust storm over East Asia for the periods 1960-2004 by Wang et al. (2008b). As shown in Fig. 7a, the highest DOF in the recent 15-year period between 1999 and 2013 was observed in the Gobi Desert, coinciding with one of the major dust sources from the above mentioned studies. In addition, the DOF was higher in the Mongolian Gobi than that in the Gobi in Inner Mongolia, especially since 2004. Not only in the Gobi Desert, but also over the other regions, the dust source showed a shift from northern China to Mongolia since 2004. In northern China, the Loess Plateau and the Hexi Corridor have also been suggested as minor dust source regions (e.g., Sun et al., 2002; Kurosaki and Mikami, 2005). However, the DOF revealed a sharp decline between 2004 and 2013 in those two regions as shown in Figs. 7e-f. Some previous researches (e.g., Qian et al., 2004; Zhu et al., 2008) argued that the eastern Inner Mongolia was one of the main dust sources in the past decades (1960s to 2000s) and may link to dust events in the downwind regions. However, a decreasing trend and low values of the DOF were found in the northeast of Inner Mongolia from 2003 to 2013. Thus, the source region of Asian dust might be changed from the northern China to the Mongolian regions.

In Mongolia, dust outbreaks were frequently occurred in the south of Altai Mountain region. A high dust storm frequency has been reported at the same region during the period 1937-1999 by Natsagdorj et al. (2003). This region with the land

cover type of desert-steppe is a dust source region in the recent decade. Additionally, a high DOF was also found in the Mongolian steppes. Being sensitive to climate changes and intense human disturbances (e.g., grazing), the Mongolia steppes appear to act as potential source regions for Asian dust (Shinoda et al., 2011).

The DOF in the Taklimakan Desert during the present study period was infrequent except for the period between 2000 and 2002. In the Taklimakan Desert, the floating dust, which was not considered in this study, has been frequently observed from March 1988 to May 2004 (Wang et al., 2005). For the seasonal variations, the peak of the DOF appeared in May, about one-month time lag than that in the Gobi Desert (Kurosaki and Mikami, 2002). In addition, dust particles emitted in the Taklimakan Desert could be blocked by the surrounding mountains and deposit in the neighboring areas (e.g., Kurosaki and Mikami, 2005), so that the Taklimakan Desert has been considered as only a local dust source, but not a major source region for the dust occurrence in the downwind regions (e.g., Kim 2008; Wang et al., 2004). Therefore, it may not have great contributions to the emission of Asian dust in the recent few years.

5.2 Anthropogenic impact in Inner Mongolia

The shift of dust source region in East Asia is primarily dependent on the erodibility as discussed in the previous section. However, the anthropogenic factors were not taken into consideration although the control on grazing has been suggested to help increase the spring vegetation in the Inner Mongolian steppes.

Due to the limitation of available data, this study now restricts analysis to the 19 stations in Inner Mongolia as indicated by the red dots in the map of Fig. 32. It also shows the time series of the DOF, SWF and DOR in April, and the above-discussed

erodibility parameters. Dust outbreaks in Inner Mongolia occurred frequently from 2000 to 2002 and in 2006. Then, the DOF declined and remained under 7% from 2007 to 2013, with a decreasing trend in the SWF. The DOR also revealed a general decreasing trend between 1999 and 2013 with inter-annual variations, indicating a reversing trend of the land surface conditions in Inner Mongolia. It is probably affected by an obvious increase in the April NDVI and the increase in spring NDVI as illustrated in the Fig. 33b. Utilizing the same regression analysis method, results in Fig. 29 show that the DOF in Inner Mongolia was under the erodibility-controlled pattern, and the most contributing erodibility factor was the NDVI in April ($r^2=0.39$, $p<0.05$).

The Chinese government launched the “Grain for Green” program in selected areas in 1999 to convert farmland to forest or grassland, and the program was expanded to the rest of the country in 2002. Figure 33a shows that the total area of fenced grassland between 1998 and 2012 in Inner Mongolia increased. It revealed a significantly positive relation with NDVI at the 5 % level as shown in Fig. 34b ($r^2=0.36$, $p<0.05$). Fencing degraded grassland can prevent over-grazing, allowing the vegetation and soil to recover (Ci and Yang 2010). In addition, the total area of cultivated land, as shown in Fig. 34c varied considerably before stabilizing in 2006. A similar plateauing of the number of sheep and goats also occurred in 2006 (Fig. 34d). This stabilization in agricultural and grazing activities may have assisted the recovery of vegetation.

Since the climate change is considered to be contributing to desertification, the present study also discussed data in Xilingol League. The administrative map is shown in Fig. 35. The Xilingol League is divided into two county-level cities, one county and nine banners. The Abaga-qi (banner) is mainly covered by typical steppe as shown in the vegetation map (Fig. 36), and its dominant economy is grazing.

In the Inner Mongolian steppe, the enclosure method and control of livestock population have been formulated to prevent the land degradation. The ratio of fenced grassland to the total grassland and the sheep unit at county basis in Xilingol League are shown in Fig. 37. In the typical steppe region, namely Abaga-qi, the ratio of fenced grassland of 57.7% at the end of 2005 increased to 96.8% in 2012. Grazing activities are forbidden in the areas of fenced grassland. The statistic data suggest that almost all pasture steppe in Abaga-qi have been prohibited from grazing. The livestock were controlled within house-feeding pattern. This leads to normal growth of the vegetation in the pasture steppe. In addition, the sheep unit reduced by 0.35 million heads. The control on grassland degradation has received success to some extent in Abaga-qi, and then its impact on vegetation has been investigated.

Figure 38 shows the inter-annual variation of NDVI, precipitation, temperature, and the ratio of fenced grassland and sheep unit in Abaga-qi. The summer precipitation amount varied between 50 and 210 mm, and the maximum NDVI is in the range of 0.25-0.55. In April, the NDVI decreased to the lowest value in 2002, and then it showed a general increasing trend between 1999 and 2013 with inter-annual variations, indicating a reversing trend of the land surface conditions in Abaga-qi. The temperature in April was above 0 degree except in 2010. As shown in Fig. 38c, trend in the ratio of fenced grassland increased from 2006 to 2013, and the sheep unit number was in the opposite trend.

The regression method was employed between NDVI and possibly related natural and anthropogenic factors. In steppe region, the summer vegetation is primarily controlled by the summer precipitation. As shown in Fig. 39a, the annual maximum NDVI in Abaga-qi was closely related to the summer precipitation amount ($r=0.66$,

$p < 0.05$). In spring, since the precipitation amount is quite low, the growth of vegetation is always dependent on temperature. Results of the regression analysis show that the NDVI in April was not dependent on the temperature in April or the annual maximum NDVI in the previous year in Abaga-qi. Therefore, the impact of human activities on the increasing trend in spring NDVI were taken into consideration. Figure 40 shows that the total area of fenced grassland had a significantly positive relation with NDVI at the 5 % level ($r = 0.71$, $p < 0.05$). The decrease in sheep unit was negatively related to the spring vegetation, but not significant at the 5 % level. As mentioned above, the spring vegetation can be protected from the control on over-grazing with the enclosure method. In Inner Mongolia, the policy of deferring spring grazing also helped increase the spring vegetation and the grassland productivity (see Section 4.2.2).

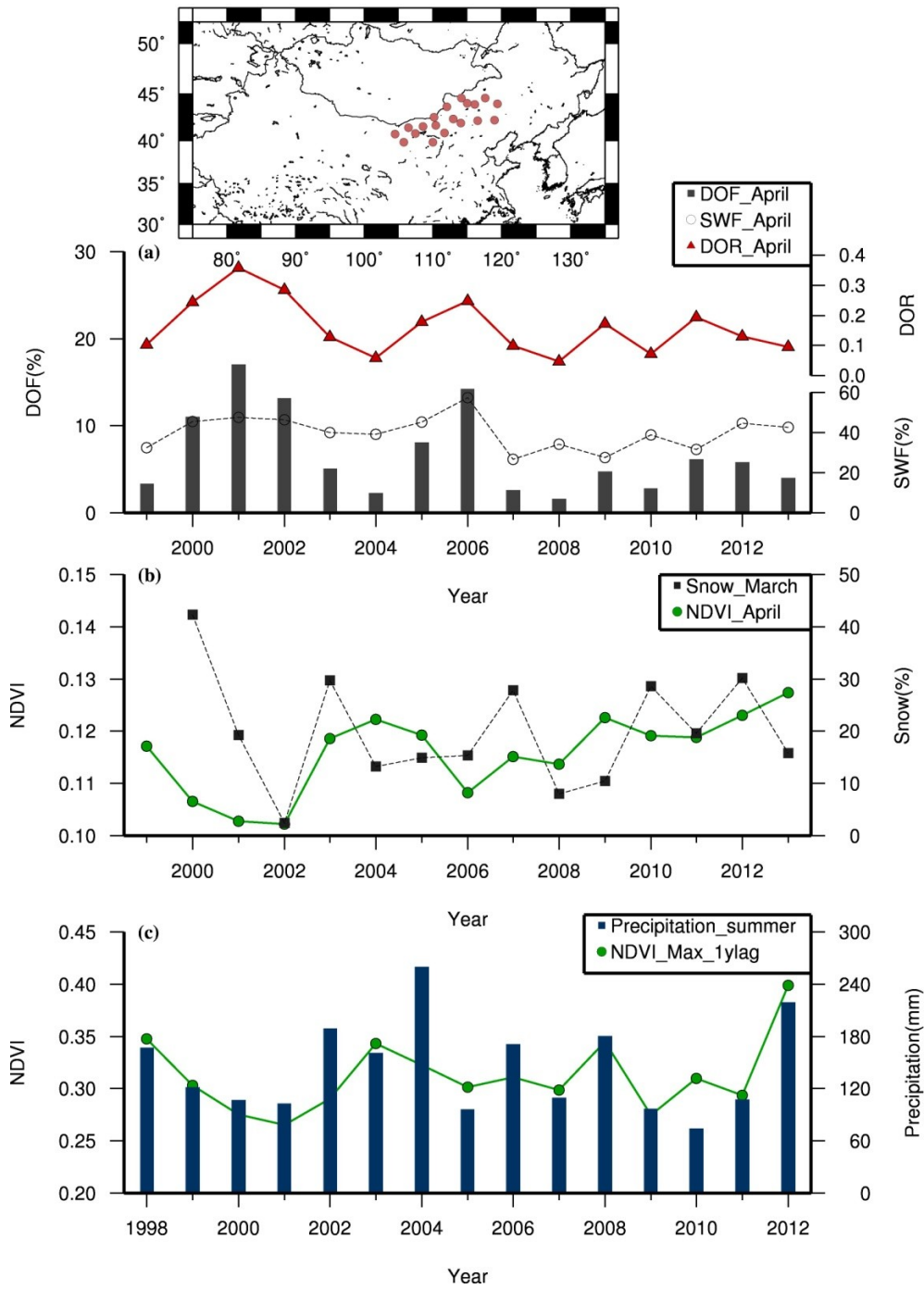


Figure 32. Inter-annual variations of (a) DOF, SWF, DOR in April, (b) NDVI in April and snow coverage in March during the period 1999-2013 and (c) summer precipitation (June to August) and annual maximum NDVI during the period 1998-2012 for the 19 stations in Inner Mongolia.

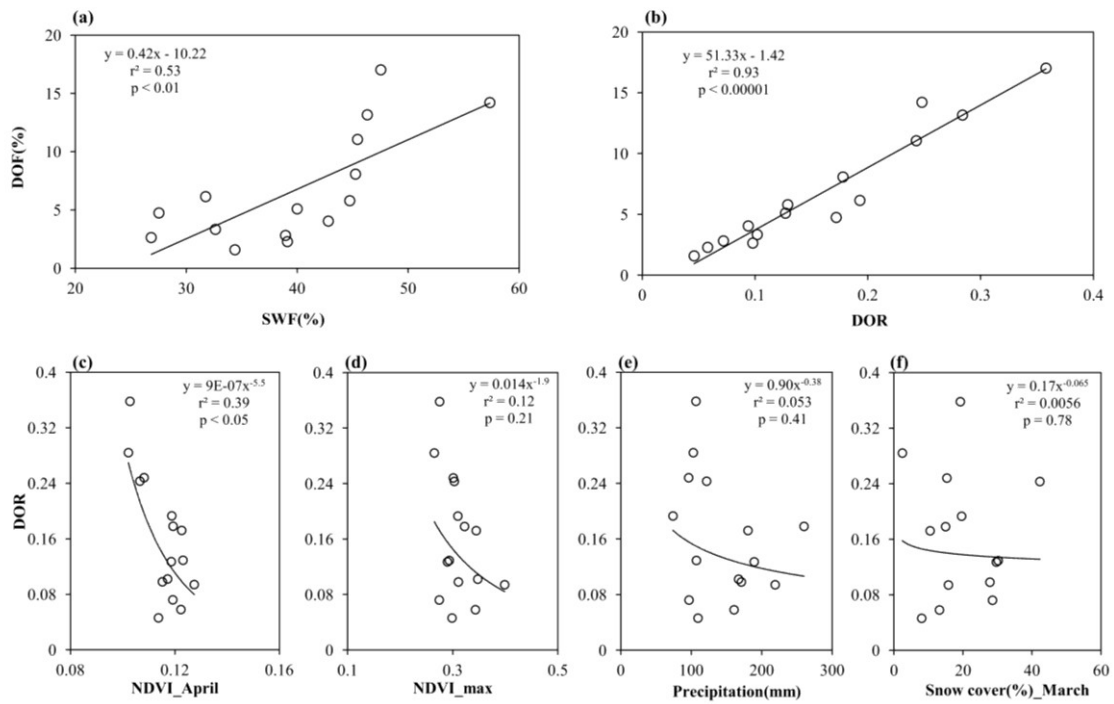


Figure 33. Same as Fig. 20 except for the station for the mean values of the 19 stations in Inner Mongolia.

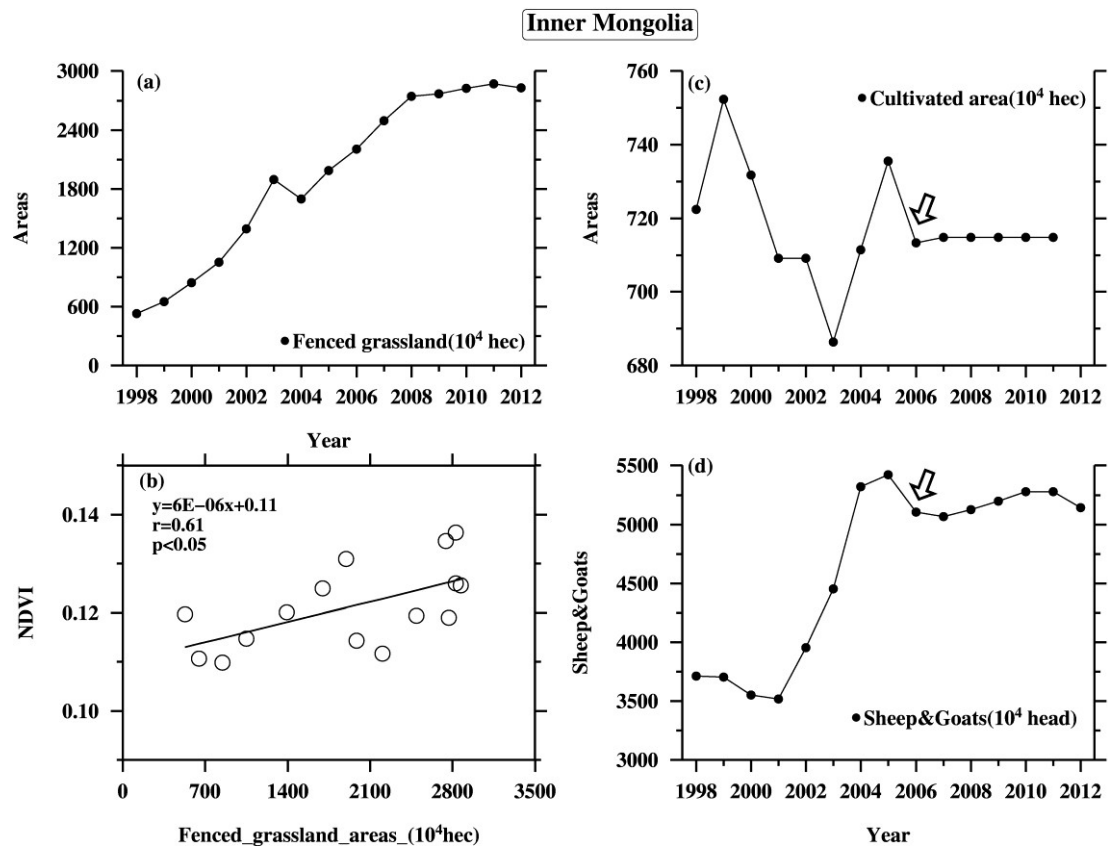


Figure 34. Inter-annual variations of (a) fenced grassland areas, (c) total cultivated land area and (d) the total number of sheep and goats at the end of the year, 1998-2012 in Inner Mongolian, and (b) plot of the April NDVI and the total area of fenced grassland in Inner Mongolia. Arrows in (c) and (d) indicate a plateauing of the variables. (Data source: Inner Mongolian Statistical Yearbook, 1999-2013).



Figure 35. Administrative map of Xilingol League.

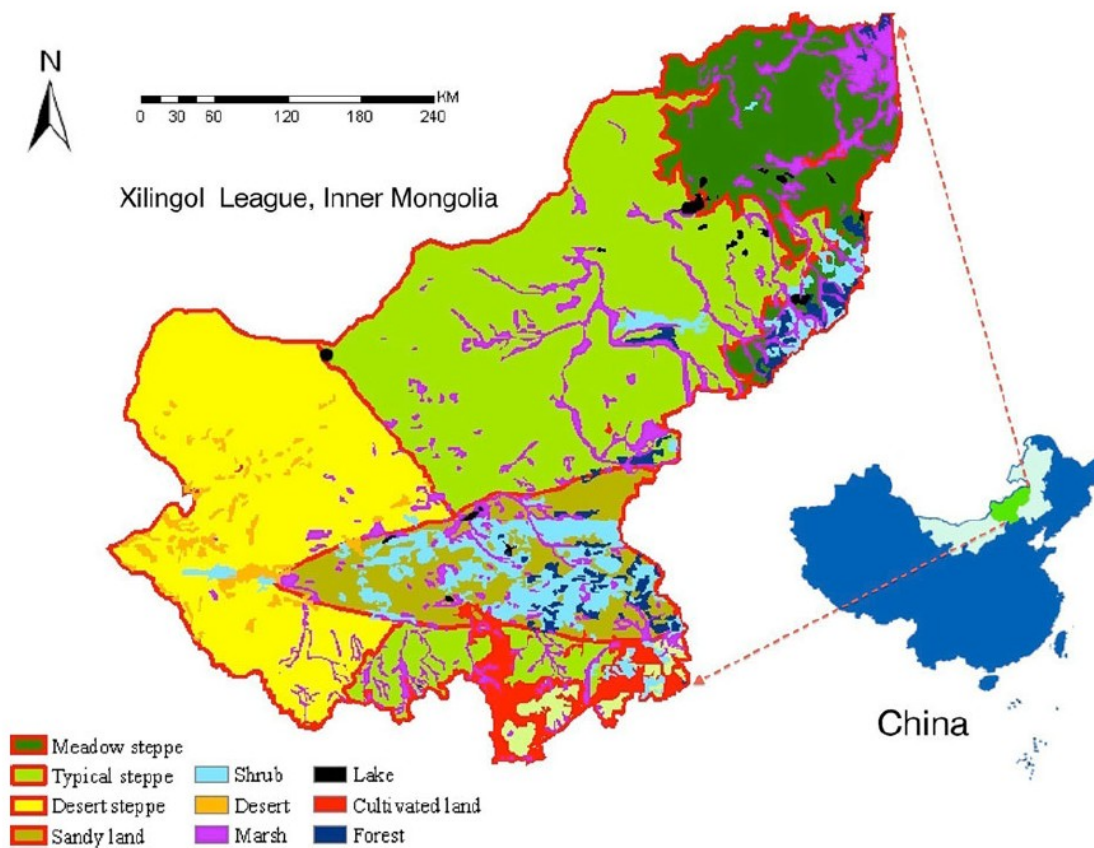


Figure 36. Vegetation map of the Xilingol grassland region, Inner Mongolia, China, showing the spatial pattern of major ecosystem types present in the 1960s–1970s (redrawn from Hou 2001).

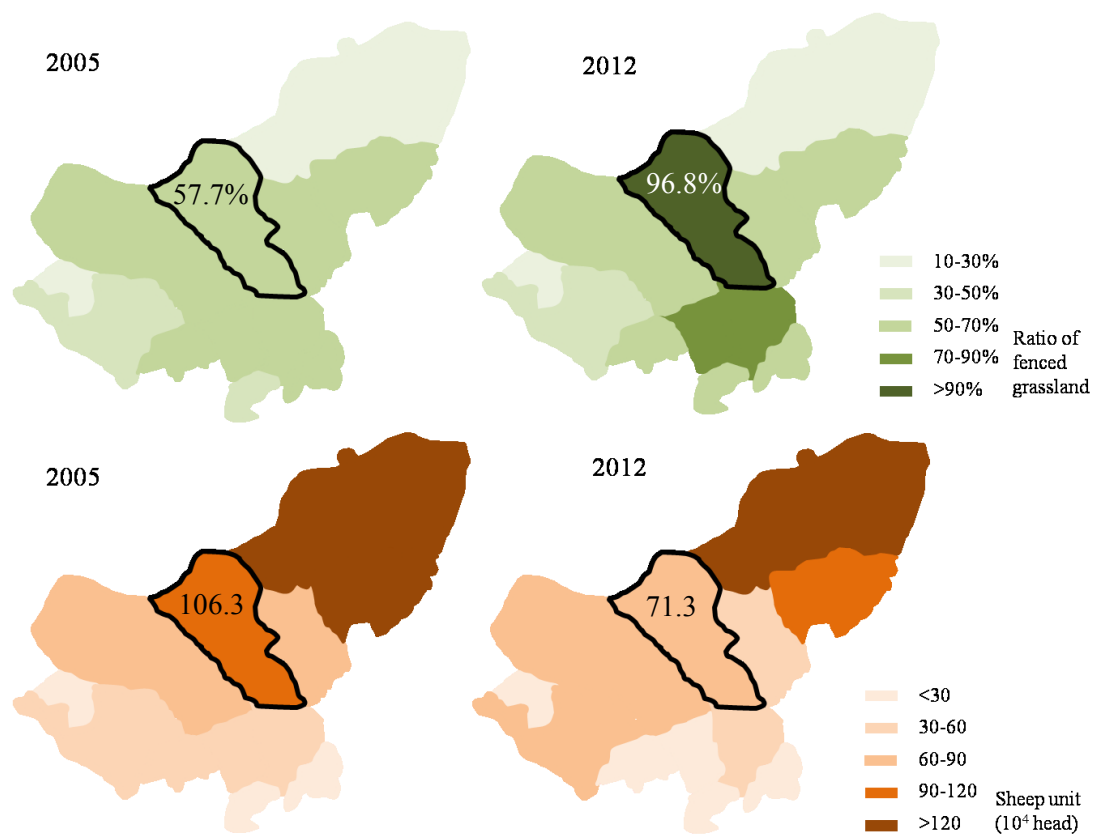


Figure 37. Distributions of the ratio of fenced grassland in Xilingol League in 2005 (a), and 2012 (b), respectively; and sheep unit in 2005 (c), and (d), respectively.

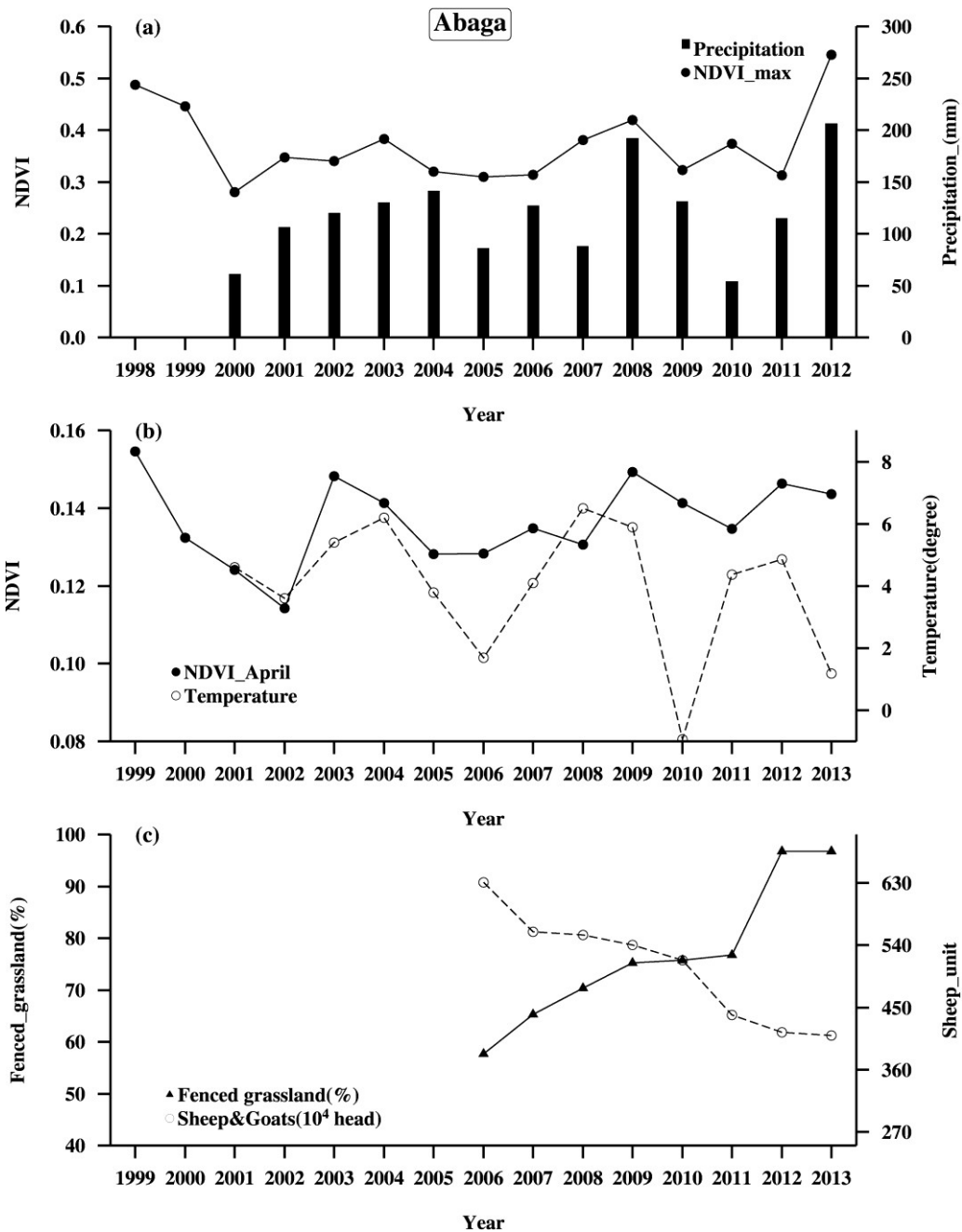


Figure 38. Inter-annual variations of (a) NDVI and precipitation in summer between 1998 and 2012, (b) NDVI and temperature in April between 1999 and 2013, and (c) the ratio of fenced grassland to the total grassland and the number of sheep unit at year end during the period 1998-2012 at Abaga Qi.

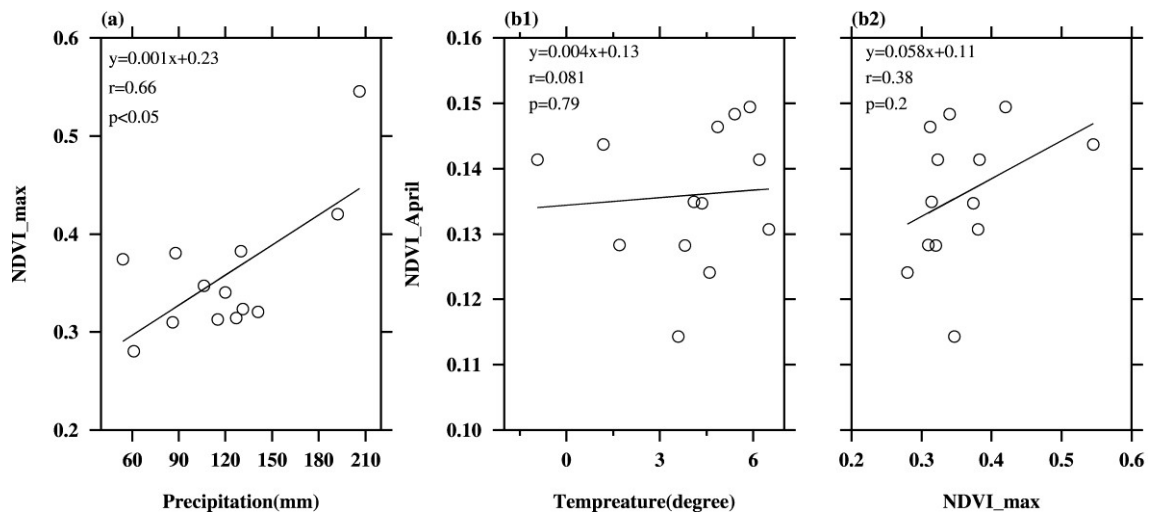


Figure 39. Scatter diagrams for (a) annual maximum NDVI and summer precipitation, NDVI in April and (b1) temperature in April, (b2) an annual maximum NDVI at Abaga Qi.

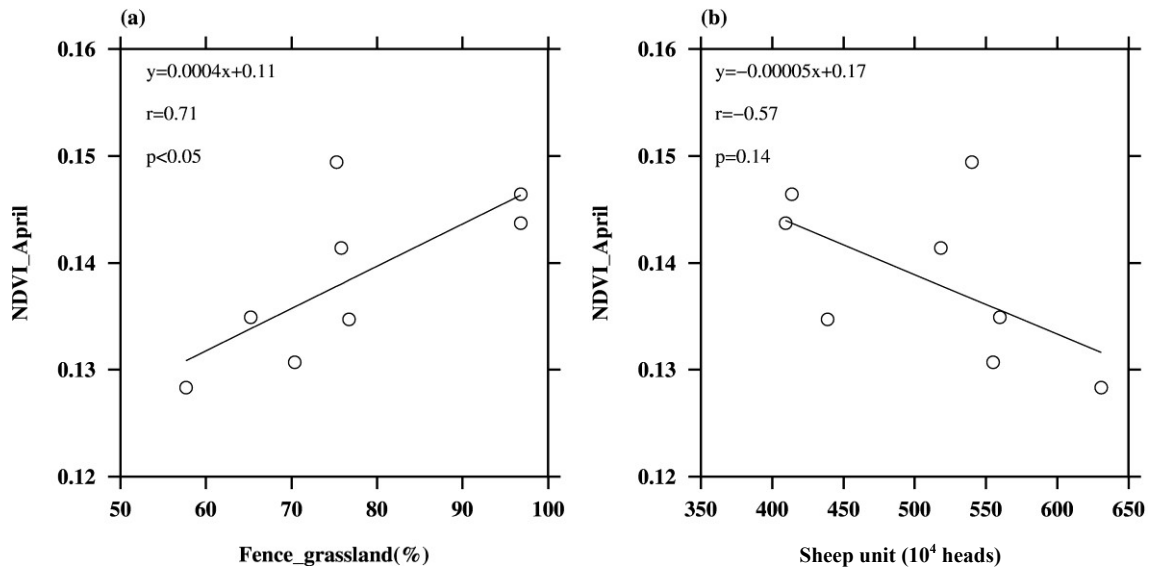


Figure 40. Scatter diagrams for the NDVI in April and (a) the ratio of fenced grassland to the total grassland, and (b) sheep unit at Abaga Qi

6. Conclusion

This study investigated the recent trend in spring dust emission, its erosivity and erodibility between 1999 and 2013 in the arid and semi-arid regions in East Asia, and identified relative contributions of the erosivity and various erodibility parameters to inter-annual dust variations on a station basis.

This study is aimed to understand the recent trend in spring dust emission, its erosivity and erodibility between 1999 and 2013 in East Asia. Generally, dust outbreaks occurred more frequently in Mongolia than in northern China. The spatial distributions were investigated to understand changes in source regions for dust outbreaks. Between 2000 and 2003, the occurrence of dust outbreaks was more frequently in northern China than in Mongolia. Large positive anomalies of strong wind were distributed in northern China during this period, and large positive anomalies of dust outbreak ratio were also found for the period of 2000 to 2002. Since the year 2004, the occurrence of dust outbreaks in northern China revealed a decreasing trend except for the year 2006 when frequent strong wind occurred. During the study period, the distribution of frequent dust outbreaks in Mongolia was widespread to the east, along with a slight increasing trend in the strong wind. The steppe region appears to be a potential dust source region. The results suggest that the source region for Asian dust shifted from northern China to Mongolia.

Contributions of erosivity and erodibility to dust emission differ substantially from region to region, depending on characteristics of land surface conditions. Kurosaki et al. (2011b) suggested that erosivity controls the DOF in the desert regions, while erodibility factors show a greater effect in other regions. The significant impact of erodibility parameters of precipitation, soil moisture, and above-ground biomass on

variations in the DOF has been investigated at only one station in Mongolia by Kurosaki et al. (2011a). Their findings have been confirmed by the present study and furthermore the previous analysis was for the first time extended to a wider dust-producing area of East Asia.

Erosivity was the major controlling factor for dust outbreaks at most stations in the Taklimakan Desert and on the north side of the Altai Mountain region. Erodibility, rather than erosivity, has a significant impact on dust outbreaks in the steppe regions. Lower precipitation or poor vegetation in the previous summer was connected to dusty springs in the Mongolian steppe. Moreover, vegetation and snow cover in spring suppressed dust outbreaks in the Inner Mongolian steppe. Anthropogenically restored vegetation in desertified areas reduced the occurrence of dust outbreaks in the Loess Plateau.

The effect of anthropogenic factors (e.g., grazing) on vegetation in Inner Mongolia is discussed. The current study suggests that the expansion of fenced grassland areas, and a plateauing of the amount of land being cultivated and the livestock population were related to the increase in the NDVI, especially from 2007 to 2013, which in turn was responsible for the recent decline in the frequency of dust outbreaks. Since climate change could be contributing to desertification, data of Abaga-qi, a county in Xilingol League of Inner Mongolia is further discussed. The results suggest that the summer vegetation in the typical steppe area were controlled by precipitation. However, the increasing trend in spring vegetation was greatly affected by the protection of vegetation by the policy of dederring spring grazing in Inner Mongolia.

Acknowledgements

I would like to express my sincere thanks and gratitude to my supervisor, Prof. Kenji Kai (Nagoya University) for his great support and contribution to my research and paper in the doctoral program. I would also like to express my great thanks to Prof. Shinoda (Nagoya University) for his thoughtful and valuable advice and comments on my research and English writing. I would like to thank Dr. Kurosaki (Arid Land Research Center, Tottori University) for his considerate support and constructive comments on the present study. I would like to thank Dr. Matsui and Dr. Nandiantsetseg (Nagoya University) for their advice and comments. I would like to thank Dr. Du for providing the statistic data of the Year Book in Inner Mongolia and Mongolia, and for her support and encourage. I wish to thank the present and former members of our laboratory for their help to my study and life in Japan.

The present study was supported by the in part by Grants-in-Aid for Scientific Research from JSPS (No.s 24340111 and 25220201), by the JSPS Core-to-Core Program (B. Asia-Africa Science Platforms), and by Budget Request of Tottori University, sponsored by special coordinate funds from the Ministry of Education, Culture, Sports, Science and Technology of the Japanese Government.

Reference

- Abulaiti A., R. Kimura, M. Shinoda, Y. Kurosaki, M. Mikami, M. Ishizuka, Y. Yamada, E. Nishihara, and B. Gantsetseg, 2014. An observational study of saltation and dust emission in a hotspot of Mongolia. *Aeolian Research*, 15, 169-176.
- Aoki, I., Y. Kurosaki, R. Osada, T. Sato, and F. Kimura, 2005: Dust storms generated by mesoscale cold fronts in the Tarim Basin, Northwest China. *Geophys. Res. Lett.*, 32, 6.
- Assembly, U. G., 1994: Elaboration of an International Convention to Combat Desertification in countries experiencing serious drought and/or desertification, particularly in Africa. *A. AC*, 241, 27.
- Chen, Y., and H. Tang, 2005: Desertification in north china: background, anthropogenic impacts and failures in combating it. *Land Degradation and Development*, 16(4), 367.
- Ci, L., and X. Yang (Eds.), 2010: Desertification and Its Control in China, 77–78 China: Higher Education Press.
- Ginoux, P., M. Chin, I. Tegen, J. M. Prospero, B. Holben, O. Dubovik, and S.J. Lin, 2001: Sources and distributions of dust aerosols simulated with the GOCART model. *J. Geophys. Res: Atmospheres* (1984–2012) 106 (D17), 20255–20273.
- Goudie, A. S., and N. J. Middleton, 1992: The changing frequency of dust storms through time. *Climatic change*, 20(3), 197-225.
- Guo, G., and G. Xie, 2008: Technical note: Dust storms in China decreased during the last 50 years. *International Journal of Remote Sensing*, 29(6), 1619–1620.
- Hall, Dorothy K., G. A. R., and V. V. Salomonson, 2006: *Updated monthly*.

- MODIS/Terra Snow Cover Daily L3 Global 0.05Deg CMG. Version5.*, Boulder, Colorado USA: National 329 Snow and Ice Data Center.
- Han, L., A. Tsunekawa, and M. Tsubo, 2011: Effect of frozen ground on dust outbreaks in spring on the eastern Mongolian Plateau. *Geomorphology*, 129(3), 412-416.
- Hara, Y., I. Uno, and Z. Wang, 2006: Long-term 281 variation of Asian dust and related climate factors. *Atmospheric Environment*, 40(35), 6730–6740.
- Ishizuka, M., M. Mikami, Y. Yamada, R. Kimura, Y. Kurosaki, D. Jugder, B. Gantsetseg, Y. Cheng, and M. Shinoda, 2012: Does ground surface soil aggregation affect transition of the wind speed threshold for saltation and dust emission?. *SOLA*, 8(0), 129-132.
- Ji, X., Z. Zhao, 2001: Preventing and controlling measures for sandstorm in Hexi Corridor according to wind-sand transport law. *Journal of Gansu Forestry Science and Technology* 26 (2), 1-5 (in Chinese).
- Kim, H.S., and K. Kai, 2007: Recent dust outbreaks in the Taklimakan desert and their relation to surface wind and land surface condition. *SOLA*, 3(0), 69–72.
- Kim, J., 2008: Transport routes and source regions of Asian dust observed in Korea during the past 40 years (1965–2004). *Atmospheric Environment*, 42(19), 4778–4789.
- Kimura, R., and M. Shinoda, 2010: Spatial distribution of threshold wind speeds for dust outbreaks in northeast Asia. *Geomorphology*, 114(3), 319–325.
- Kimura, R., 2012a: Effect of the strong wind and land cover in dust source regions on the Asian dust event over Japan from 2000 to 2011. *SOLA*, 8(0), 77-80.
- Kimura, R., 2012b: Factors contributing to dust storms in source regions producing the yellow-sand phenomena observed in Japan from 1993 to 2002. *Journal of Arid*

Environments, 80, 40–44.

Kurosaki, Y., and M. Mikami, 2003: Recent frequent dust events and their relation to surface wind in East Asia. *Geophysical Research Letters*, 30(14).

Kurosaki, Y., and M. Mikami, 2005: Regional difference in the characteristic of dust event in East Asia: relationship among dust outbreak, surface wind, and land surface, *J. Meteor. Soc. Japan*, 83A, 1–18.

Kurosaki, Y., and M. Mikami, 2007: Threshold wind speed for dust emission in East Asia and its seasonal variations. *J. Geophys. Res.*, **112**, D17202, doi:10.1029/2006JD007988.

Kurosaki, Y., M. Shinoda, M. Mikami, and B. Nandintsetseg, 2011: Effects of soil and land surface conditions in summer on dust outbreaks in the following spring in a Mongolian grassland. *SOLA*, 7, 69-72.

Lee, E. H., and B. J. Sohn, 2011: Recent increasing trend in dust frequency over mongolia and inner mongolia regions and its association with climate and surface condition change. *Atmospheric Environment*, 45(27), 4611–4616.

Lee, J. J., and C. H. Kim, 2012: Roles of surface wind, NDVI and snow cover in the recent changes in Asian dust storm occurrence frequency. *Atmos. Environ*, 59, 366-375.

Liu, X., Z.Y. Yin, X. Zhang, and X. Yang, 2004: Analyses of the spring dust storm frequency of northern China in relation to antecedent and concurrent wind, precipitation, vegetation, and soil moisture conditions. *J. Geophys. Res.*, 109(D16), D16210.

Miller, R., and I. Tegen, 1998: Climate response to soil dust aerosols. *J. Clim.*, 11(12), 3247–3267.

- Myneni, R. B., C. D. Keeling, C. J. Tucker, G. Asrar, and R. R. Nemani, 1997:
Increased plant growth in the northern high latitudes from 1981-1991. *Nature*, 386,
698–702.
- Natsagdorj, L., D. Jugder, and Y. Chung, 2003: Analysis of dust storms observed in
Mongolia during 1937–1999. *Atmos. Environ.*, 37(9), 1401–1411.
- Nandintsetseg, B., and M. Shinoda, 2015: Land surface memory effects on dust
emission in a Mongolian temperate grassland. *J. Geophys. Res.: Biogeosci.*, 120(3),
414-427.
- Pettorelli, N., J. O. Vik, A. Mysterud, J. M. Gaillard, C. J. Tucker, and N. Stenseth,
2005: Using the satellite-derived 319 ndvi to assess ecological responses to
environmental change. *Trends in Ecology and Evolution*, 20, 503–510.
- Prospero, J. M., P. Ginoux, O. Torres, S. E. Nicholson, and T. E. Gill, 2002:
Environmental characterization of global sources of atmospheric soil dust
identified with the Nimbus 7 Total Ozone Mapping Spectrometer (TOMS)
absorbing aerosol product. *Reviews of geophysics*, 40(1), 2-1.
- Qian, W., L. Quan, and S. Shi, 2002: Variations of the dust storm in china and its
climatic control. *Journal of Climate*, 15(10), 1216–1229.
- Qian, W., X. Tang, and L. Quan, 2004: Regional characteristics of dust storms in China.
Atmospheric Environment, 38(29), 4895-4907.
- Qi, J., J. Chen, S. Wan., and L. Ai 2012: Understanding the coupled natural and human
systems in Dryland East Asia. *Environ. Res. Lett*, 7(1), 015202.
- Shao, Y., and C. H. Dong, 2006: A review on East Asian dust storm climate, modelling
and monitoring. *Global and Planetary Change*, 52(1), 1-22.
- Shao, Y., and J. Wang, 2003: A climatology of Northeast Asian dust events.

Meteorologische Zeitschrift, 12(4), 187-196.

Shinoda, M., J. Gillies, M. Mikami, and Y. Shao, 2011: Temperate grasslands as a dust source: Knowledge, uncertainties, and challenges. *Aeolian Res.*, 3(3), 71–293.

Shinoda, M., and B. Nandintsetseg, 2011: Soil moisture and vegetation memories in a cold, arid climate. *Glob. Planet. Chang.*, 79(1), 110-117.

Takemi, T., and N. Seino, 2005: Dust storms and cyclone tracks over the arid regions in east Asia in spring. *J. Geophys. Res: Atmospheres* 110, D18S11, doi:10.1029/2004JD004698.

Tan, M., and X. Li, 2015: Does the green great wall effectively decrease dust storm intensity in China? A study based on NOAA NDVI and weather station data. *Land Use Policy*, 43, 42–47.

Tegen, I., and I. Fung, 1994: Modeling of mineral dust in the atmosphere: Sources, transport, and optical thickness. *Journal of Geophysical Research: Atmospheres (1984–2012)*, 99(D11), 22897–22914.

Todd, M., D. Karam, C. Cavazos, C. Bouet, B. Heinold, J. Baldasano, G. Cautenet, I. Koren, C. Perez, F. Solmon, I. Tegen, P. Tulet, R. Washington, and A. Zakey, 2008: Quantifying uncertainty in estimates of mineral dust flux: An intercomparison of model performance over the Bodélé Depression, northern Chad. *J. Geophys. Res: Atmospheres (1984–2012)*, 113(D24).

Tucker, C., and P. Sellers, 1986: Satellite remote sensing of primary production. *International Journal of Remote Sensing*, 7(11), 1395–1416.

Veroustraete, F., E. Bartholome, and W.W. Verstraeten, 2005: Operational early warning system using spotvegetation and terra-modis to predict desert locust outbreaks. *Proceedings of the Second International VEGETATION User Conference* 33–41.

- United Nations Environment Programme, 1997: World Atlas of desertification, 2nd ed., edited by N. J. Middleton and D. S. G. Thomas, Edward Arnold, London.
- Uno, I., Z. Wang, M. Chiba, Y. Chun, S. Gong, Y. Hara, E. Jung, S.S. Lee, M. Liu, M. Mikami, S. Music, S. Nickovic, S. Satake, Y. Shao, Z. Song, N. Sugimoto, T. Tanaka, and D. Westphal, 2006: Dust model intercomparison (dmip) study over Asia: Overview, *J. Geophys. Res.*, 111, D12213, doi:12210.11029/12005JD006575.
- Wang, T., W. Wu, X. Xue, W. Zhang, Z. Han, and Q. Sun, 2003: Time-space evolution of desertification land in northern China. *Journal of Desert Research*, 23(3), 230-235 (in Chinese with English abstract).
- Wang, S., J. Wang, Z. Zhou, and K. Shang, 2005: Regional characteristics of three kinds of dust storm events in China. *Atmos. Environ*, 39(3), 509-520.
- Wang, X., F. Chen, E. Hasi, and J. Li, 2008a: Desertification in china: an assessment. *Earth-Science Reviews*, 88(3), 188–206.
- Wang, X., J. Huang, M. Ji, and K. Higuchi, 2008b: Variability of East Asia dust events and their long-term trend. *Atmospheric Environment*, 42(13), 3156–3165.
- Wang, X., Z. Dong, J. Zhang, and L. Liu, 2004: Modern dust storms in China: an overview. *Journal of Arid Environments*, 58(4), 559-574.
- Woodage, M., A. Slingo, S. Woodward, and R. Comer, 2010: UK HiGEM: simulations of desert dust and biomass burning aerosols with a high-resolution atmospheric GCM. *J. Clim.*, 23(7), 1636-1659.
- World Meteorological Organization, 1995: *Manual on Codes, International Codes, vol. I.1 (Annex II to WMO Technical Regulations), part A, Alphanumeric Codes*. Geneva, Switzerland.
- Xu, X., J. K. Levy, L. Zhaohui, and C. Hong, 2006: An investigation of sand–dust storm

- events and land surface characteristics in china using NOAA NDVI data. *Glob. Planet. Chang.*, 52(1), 182–196.
- Zhang, B., A. Tsunekawa, and M. Tsubo, 2008: Contributions of sandy lands and stony deserts to long-distance dust emission in China and Mongolia during 2000–2006. *Global and Planetary Change*, 60(3), 487-504.
- Zhang, X. Y., S. L. Gong, T. L. Zhao, R. Arimoto, Y. Q. Wang, and Z. J. Zhou, 2003: Sources of Asian dust and role of climate change versus desertification in Asian dust emission. *Geophysical Research Letters*, 30(24).
- Zhang, X. Y., and S. L. Gong, 2005: Contribution of the anthropogenic desertification in China to Asian dust storm. *Adv. Clim. Change Res*, 1, 147-150.
- Zhu, C., B. Wang, and W. Qian, 2008: Why do dust storms decrease in northern China concurrently with the recent global warming? *Geophysical Research Letters*, 35(18).
- Zou, X. K., and P. M. Zhai, 2004: Relationship between vegetation coverage and spring dust storms over northern china. *J. Geophys. Res: Atmospheres (1984–2012)*, 109(D3).